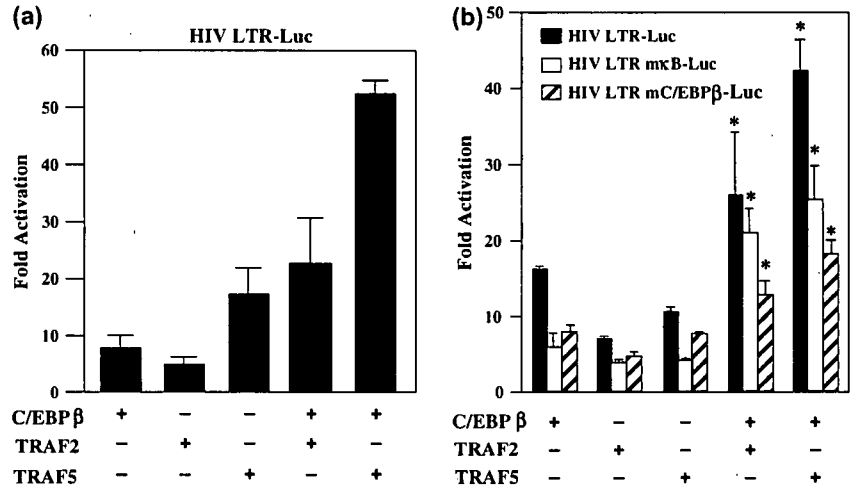

Fig. 2. Potentiation of C/EBPβ-mediated HIV-LTR activation by TRAF. (a) Effects of TRAF on C/EBPβ-mediated induction of HIV-LTR. (b) Effects of mutations in NF-κB or C/EBPβ sites of HIV-LTR on C/EBPβ-mediated HIV-LTR activation by TRAF. Transient co-transfection reporter gene assay was done in U937 cells using HIV-LTR-Luc, HIV-LTR mκB-Luc or HIV-LTR mC/EBPβ-Luc as reporters. Twenty five nanograms of reporter construct and 100 ng of pRL-TK were co-transfected into 1×10^5 cells with expression plasmids of TRAF2, TRAF5 or C/EBPβ (50 ng each). Total amount of DNA transfected was adjusted to 550 ng by an empty expression vector. Levels of activation are expressed as fold activation compared with the basal luciferase activity of the reporter constructs. Bars indicate standard deviation. $^*P < 0.05$.

mκB-Luc) (Fig. 2b). However, this effect was not completely abolished when two C/EBPβ sites in HIV-LTR-Luc were mutated (HIV-LTR mC/EBPβ-Luc). Collectively, these results indicate that signals downstream of TRAF2 and TRAF5 can potentiate C/EBPβ-mediated activation of HIV-LTR in U937 cells and that this potentiation is not completely dependent on C/EBPβ sites in HIV-LTR.

3.3. Activation of p38 MAP kinase by TRAF signaling pathway

In addition to IKK activation that leads to NF-κB activation, TRAF2 is also involved in signaling to activate other MAP kinase kinase kinases (MAPKKK), MEKK1 and ASK1, which leads to activation of stress-activated kinase (SAPK)/c-jun N-terminal kinase (JNK) and p38 MAPK [19]. On the other hand, C/EBPβ has a consensus motif for p38 MAPK phosphorylation and was shown to be a direct target of p38 MAPK in 3T3-L1 cells [20]. Therefore, we next tested the possibility that TRAF signals activate C/EBPβ through p38 MAPK pathway. For this purpose, we examined whether p38 MAPK activated by TRAF signals can phosphorylate C/EBPβ.

We prepared a GST-C/EBPβ fusion protein that contains the consensus site of p38 MAPK for a substrate of in vitro kinase assay. p38 MAPK immunoprecipitated from anisomycin-treated U937 cells directly phosphorylated GST-C/EBPβ (Fig. 3, lane 2). It was also shown that overexpression of TRAF2 or TRAF5 in U937 can activate p38 MAPK and phosphorylate GST-C/EBPβ (Fig. 3, lanes 5 and 6). Experiments using U937 cells transfected with expression vectors for CD30, a member of TNF receptor family and truncated mutants of CD30 lacking the TRAF interacting domain also showed that p38 MAPK is activated by TNF receptor family signaling pathway (Fig. 3, lanes 3 and 4). Taken together, these results demonstrate that C/EBPβ can be activated by TRAF-p38 MAPK signaling pathway.

3.4. p38 MAPK potentiates C/EBPβ-mediated activation of HIV-1 by TRAF signals

We next examined whether p38 MAPK mediates the synergistic effects of TRAF signals on C/EBPβ-mediated activation of HIV-LTR using a p38 MAPK specific inhibitor, SB203580. In transient co-transfection studies using U937 cells, potentiation of HIV-LTR activation by C/EBPβ observed with overexpression of TRAF2, TRAF5 or CD30 was dose-dependently inhibited by addition of SB203580 (Fig. 4a). In co-transfection of C/EBPβ with TRAF2 or CD30, addition of 40 μM of SB203580 almost abolished potentiating effects on HIV-LTR

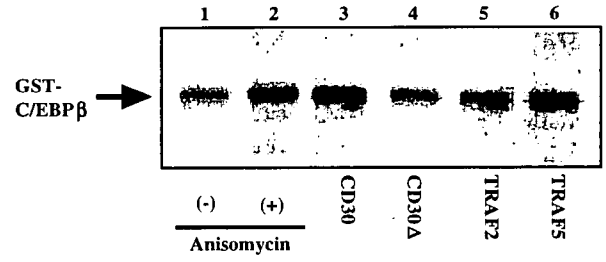

Fig. 3. p38 MAPK-mediated phosphorylation of C/EBPβ by TRAF2 and TRAF5: in vitro kinase assay. Using U937 cells, activation of p38 MAPK by TRAF2, TRAF5 and CD30 was studied by in vitro kinase assay using C/EBPβ as a substrate. U937 cells treated with or without anisomycin (10 μg/ml for 20 min) served as a positive or negative control, respectively. CD30; wild type of CD30, CD30Δ; CD30 lacking binding domain for TRAF2 and TRAF5.

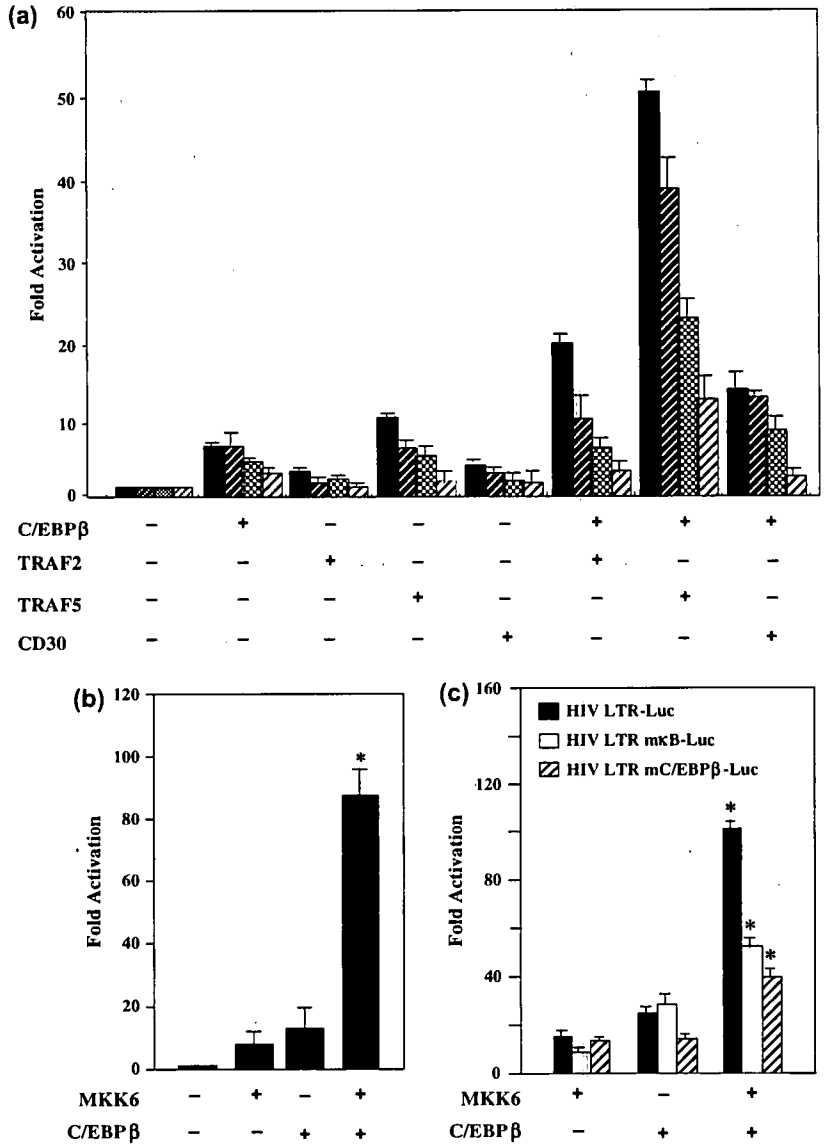

Fig. 4. p38 MAPK is involved in the potentiation of C/EBPβ by TRAF signals. (a) Effects of p38 MAPK inhibitor SB203580 on potentiation of CEBPβ mediated HIV-LTR induction by TRAF2, TRAF5 or CD30. Transient co-transfection reporter gene assay was done in 1×10^5 U937 cells using HIV-LTR-Luc constructs (25 ng) as a reporter and indicated expression plasmids for TRAF2, TRAF5 or CD30 (50 ng each) with or without indicated concentration of SB203580. One hundred nanograms of pRL-TK was also transfected to standardize the transfection efficiency. Total amount of DNA transfected was adjusted to 550 ng by an empty expression vector. Levels of activation are expressed as fold activation compared with the basal luciferase activity of the reporter constructs. Bars indicate standard deviation. (b) Effects of MKK6 on C/EBPβ-mediated induction of HIV-LTR. Transient co-transfection reporter gene assay was done in U937 cells using HIV-LTR-Luc as a reporter. Twenty five nanograms of reporter construct was co-transfected into 1×10^5 cells with an expression plasmid for MKK6 or C/EBPβ (50 ng each). One hundred nanograms of pRL-TK was also transfected to standardize the transfection efficiency. In each experiment total amount of DNA transfected was adjusted to 225 ng by an empty expression vector. Levels of activation are expressed as fold activation compared with the basal luciferase activity of the reporter constructs. Bars indicate standard deviation. $^*P < 0.05$. (c) Effects of mutations in NF-κB or C/EBPβ sites of HIV-LTR on C/EBPβ-mediated HIV-LTR activation by MKK6. Transient co-transfection reporter gene assay was done in U937 cells using HIV-LTR mκB-Luc or HIV-LTR mC/EBPβ-Luc as reporters. The experiment was performed as described in the legend for Fig. 4b. Bars indicate standard deviation. $^*P < 0.05$.

activation, whereas in co-transfection of C/EBPβ with TRAF5 suppression of the synergistic effect by SB203580 was incomplete even at the concentration of 40 μM where HIV-LTR was activated more than 10-fold (Fig. 4a). This suggests that another pathway may also be involved in C/EBPβ activation by TRAF5, which remains to be clarified. Collectively, our results strongly suggest that synergistic effects observed in HIV-LTR activation by C/EBPβ and TRAF signals are mediated mainly by p38 MAPK-mediated activation of C/EBPβ.

We further tested whether direct activation of p38 MAPK by MKK6 potentiates C/EBPβ-mediated activation of HIV-LTR. MKK6 is a MAPK kinase (MAPKK), which directly

and specifically activates p38 MAPK [21]. In transient co-transfection assays using U937 cells, overexpression of C/EBPβ and MKK6 showed a marked activation of HIV-LTR (Fig. 4b). This synergism was still observed when we used HIV-LTR-Luc with mutations in both NF-κB sites (HIV-LTR mκB-Luc) or HIV-LTR-Luc with mutations in both C/EBPβ sites (HIV-LTR mC/EBPβ-Luc), although the magnitude of activation was a little less than that with intact NF-κB or C/EBPβ sites (Fig. 4c). The result indicates that p38 MAPK is involved in C/EBPβ-mediated activation of HIV-LTR and suggests the notion that this activation is not completely restricted by C/EBPβ sites in HIV-LTR.

To examine involvement of p38 MAPK in reactivation of the integrated HIV by TRAF signals, we next studied the effects of SB203580 on induction of HIV p24 expression in U1 cells by CD30 and TNF receptor signals. Activation of CD30 and TNF receptor resulted in two-fold induction of p24 production by U1 cells, which was blocked by inhibition of p38 MAPK (Fig. 5).

3.5. The expression of TRAF proteins in the spleen monocytes/macrophages of HIV-1 infected patients

Although TRAF proteins have been reported to be expressed in various tissues [9], their expression in monocytes/macrophages of HIV-1 infected patients has not been reported. Therefore, we examined the expression of TRAF2 and TRAF5 in monocytes/macrophages of spleen samples from HIV-1 infected patients by immunostaining. CD68 was used to identify monocytes/macrophages. Analysis by immunofluorescence confocal microscopy revealed that cells stained by CD68 also express TRAF2 or TRAF5 ($n = 5$), suggesting monocytes/macrophages of patients infected with HIV-1 expresses TRAF proteins (Fig. 6). The result supports the notion that TRAF signals can operate in the monocytes/macrophages of the patients infected with HIV-1.

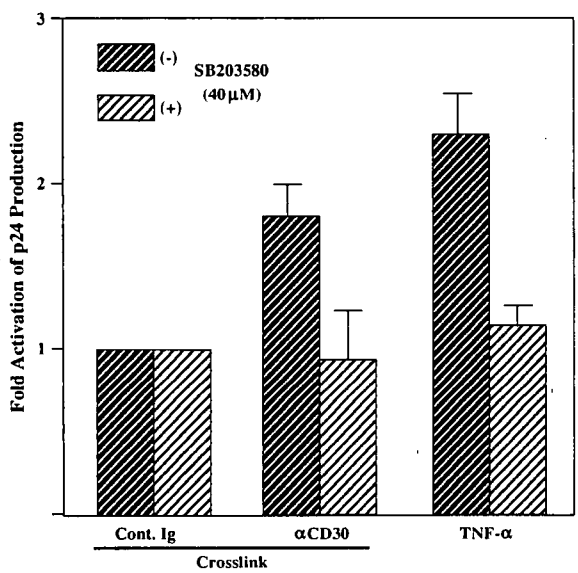

Fig. 5. Signals by TNF receptor family receptor can induce HIV-1 in U1 cells carrying latently infected HIV-1. The effects of SB203580 on induction of HIV p24 in U1 cells by CD30 and TNF receptor signals were examined by ELISA for HIV-1 p24. 1×10^6/ml of U1 cells were cross-linked by CD30 or treated with 10 ng/ml of TNFα with or without 40 μM of p38 MAPK inhibitor SB203580 for 48 h. Isotype matched IgG served as a control for cross-linking by CD30. Results of triplicated experiments are shown with standard deviation. Experiments were repeated at least three times and representative results are shown with standard deviation (s.d.). $^*P < 0.05$.

4. Discussion

In the present study, we have focused on the signal transduction pathway of TRAF other than NF-κB activation pathway in monocytes/macrophages and the results clearly showed that C/EBPβ is a target molecule of p38 MAPK activated by TRAF signals, providing evidence for another pathway of TRAF signals other than NF-κB activation to induce HIV gene expression in monocytes/macrophages.

Our initial data that TRAF activation of HIV-LTR with mutations in both NF-κB sites led us to study signaling pathways other than that for NF-κB. Involvement of p38 MAPK in activation of HIV-LTR has been documented and C/EBPβ transcription factor was shown to be involved in the activation of HIV-LTR in U937 cells [12,15,22]. Furthermore, activities of C/EBP family transcription factors are regulated by phosphorylation by MAPK. For example, CHOP was shown to be activated by p38 MAPK [23]. Another example is C/EBPβ that is activated by ras-signaling pathway, which was assumed to be mediated by ERK [24]. C/EBPβ and C/EBPδ have been reported to be regulated by phosphorylation dependent manner [25,26]. These backgrounds prompted us to focus on p38 MAPK and C/EBPβ, and test whether these molecules were involved in TRAF mediated activation of HIV-LTR.

Our results show the importance of TRAF-p38 MAPK-C/EBPβ pathway in activation of HIV-LTR in monocytes/macrophages. C/EBP factors can associate with members of the NF-κB/Rel family, generating C/EBP-NF-κB complexes, which efficiently activate transcription of cellular genes [27]. Accordingly, both the C/EBP and NF-κB *cis* sequences have been identified in the regulatory regions of many genes involved in inflammation and immune regulation [28]. In HIV-LTR, two NF-κB sites and two CEBPβ sites are also located in a neighboring region. Therefore, NF-κB and CEBPβ can be assumed to cross-talk and co-operate each other in HIV-LTR activation, as was indicated by previous reports [15,29]. Our data presented in Figs. 2b and 4c indicate induction of HIV-LTR mediated by C/EBPβ is dependent not only on C/EBPβ sites but also on NF-κB sites, supporting the notion that C/EBPβ can also activate HIV-LTR in association with NF-κB. However, this redundancy does not minimize the role of TRAF-C/EBPβ pathway in induction of HIV-LTR. The inhibition of p38 MAPK pathway significantly reduced the levels of TRAF-C/EBPβ-mediated activation of HIV-LTR (Fig. 4a), and inhibition of p38 MAPK almost completely abrogated CD30- and TNFR-signal mediated induction of HIV-1 in U1 cells (Fig. 5). Furthermore, previous reports showed that replication of HIV-1 requires C/EBPβ in

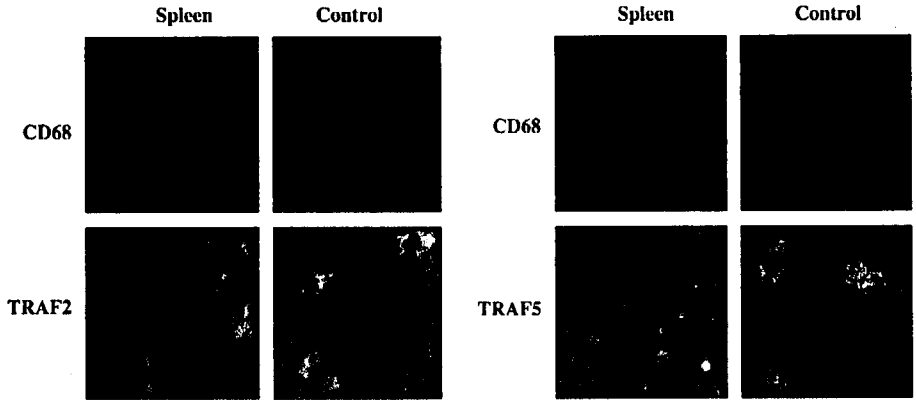

Fig. 6. The spleen macrophages of HIV-1 infected patients express TRAF2 and TRAF5. Spleen samples from HIV-1 infected patients were immunostained by TRAF2 or TRAF5 (green) and monocytes/macrophages marker CD68 (red), and observed by confocal immunofluorescence microscopy. The staining of normal tonsil served as a control.

monocytes/macrophages [13,14]. These observations strongly support the pivotal roles of TRAF-p38 MAPK-C/EBPβ pathway in HIV-LTR activation in monocytes/macrophages.

The data presented in this study also suggested that C/EBPβ is regulated by p38 MAPK dependent phosphorylation. It is well established that regulation of phosphorylation state is an important regulatory mechanism for function of transcription factors, including C/EBPβ. Multiple phosphorylation sites have been characterized on C/EBPβ and are reported to be phosphorylated by Ras signals (Thr 235), calcium/calmodulin-dependent protein kinase (Ser 276), protein kinase C (Ser 105, Ser 240, and Ser 299) and protein kinase A (Ser 105, Ser 173, Ser 233, and Ser 299) [25,26,30]. These reports indicate that multiple phosphorylation sites on C/EBPβ are available for its regulation. Our study added another example of the signal, which phosphorylates and regulates C/EBPβ function, although detailed analyses of phosphorylation sites remain to be done.

We showed that p38 MAPK is involved in the induction of HIV p24 in U1 cells by TNF receptor family signals. U1 cell line, which is chronically infected with HIV-1, is a derivative of monocytic cell line, U937 and carries latently infected HIV-1. Chronically HIV-1 infected cell lines have been used as a model for studying HIV-1 latency and reactivation. The results indicate that TRAF-p38 MAPK-C/EBPβ pathway is involved in the reactivation of the latently infected HIV-1 in monocytes/macrophages. We also showed that TRAF2 and 5 are expressed in monocytes/macrophages of spleen samples from HIV-1 infected patients. Collectively, these results indicate that the signal transduction pathway leading to HIV-1 LTR reactivation that consists of TRAF-p38 MAPK-C/EBPβ operates in monocytes/macrophages of HIV-1 infected patients.

This study underscores the significance of p38 MAPK-C/EBPβ pathway in reactivation of HIV-1 and suggests that p38 MAPK-C/EBPβ pathway is the potential target of prevention of HIV-1 reactivation in monocytes/macrophages. Recent understandings for the pathogenesis of HIV-1, and the virological and immunological responses to HAART, along with the numerous drawbacks of HAART, have clearly demonstrated that the eradication of the virus is not a feasible therapeutic goal, and that there is an urgent need to develop other approaches to control HIV-1 infection and obtain clinical benefit. Several attempts for this purpose include the use of immunosuppressive drugs as an adjuvant to HIV-1 treatment [31]. To this end, molecularly targeted treatments based on understanding of molecules involved in the reactivation of the virus from the reservoir pool will be required for efficient regulations of latent virus after interruption of HAART. The results of this study propose the TRAF-p38 MAPK-C/EBPβ pathway as a potential target of intervention in HIV-1 reactivation by compounds with low molecular weight.

In conclusion, the results in this study indicate an alternative new signal transduction pathway of TRAF proteins leading to HIV-1 LTR activation that consists of TNF receptor family-TRAF-p38 MAPK-C/EBPβ. Identification of a new pathway of TRAF signals that activate C/EBPβ, a key cellular transcription factor regulating HIV-LTR, provides a new target for controlling reactivation of latent HIV-1 in monocytes/macrophages.

References

[1] F.J. Palella Jr., K.M. Delaney, A.C. Moorman, M.O. Loveless, J. Fuhrer, G.A. Satten, D.J. Aschman, S.D. Holmberg, Declining morbidity and mortality among patients with advanced human immunodeficiency virus infection. HIV Outpatient Study Investigators, N. Engl. J. Med. 338 (1998) 853–860.

[2] T.W. Chun, A.S. Fauci, Latent reservoirs of HIV: obstacles to the eradication of virus, Proc. Natl. Acad. Sci. U.S.A. 96 (1999) 10958–10961.

[3] O. Kutsch, E.N. Benveniste, G.M. Shaw, D.N. Levy, Direct and quantitative single-cell analysis of human immunodeficiency virus type 1 reactivation from latency, J. Virol. 76 (2002) 8776–8786.

[4] M. Mallardo, E. Dragonetti, F. Baldassarre, C. Ambrosino, G. Scala, I. Quinto, An NF-kappaB site in the 5′-untranslated leader region of the human immunodeficiency virus type 1 enhances the viral expression in response to NF-kappaB-activating stimuli, J. Biol. Chem. 271 (1996) 20820–20827.

[5] R. Lapointe, R. Lemieux, A. Darveau, HIV-1 LTR activity in human CD40-activated B lymphocytes is dependent on NF-kappaB, Biochem. Biophys. Res. Commun. 229 (1996) 959–964.

[6] O. Kutsch, D.N. Levy, B.R. Kosloff, G.M. Shaw, E.N. Benveniste, CD154-CD40-induced reactivation of latent HIV-1 infection, Virology 314 (2003) 261–270.
[7] P. Biswas, C.A. Smith, D. Goletti, E.C. Hardy, R.W. Jackson, A.S. Fauci, Cross-linking of CD30 induces HIV expression in chronically infected T cells, Immunity 2 (1995) 587–596.
[8] M.A. Munoz-Fernandez, J. Navarro, A. Garcia, C. Punzon, E. Fernandez-Cruz, M. Fresno, Replication of human immunodeficiency virus-1 in primary human T cells is dependent on the autocrine secretion of tumor necrosis factor through the control of nuclear factor-kappa B activation, J. Allergy Clin. Immunol. 100 (1997) 838–845.
[9] R.H. Arch, R.W. Gedrich, C.B. Thompson, Tumor necrosis factor receptor-associated factors (TRAFs)—a family of adapter proteins that regulates life and death, Genes Dev. 12 (1998) 2821–2830.
[10] G. Herbein, Cytokines, viruses and macrophages: an interactive network. An immune dysregulation involving the members of the tumor necrosis factor (TNF) receptor superfamily could be critical in AIDS pathogenesis, Pathol. Biol. (Paris) 45 (1997) 115–125.
[11] J.M. Orenstein, C. Fox, S.M. Wahl, Macrophages as a source of HIV during opportunistic infections, Science 276 (1997) 1857–1861.
[12] P.S. Cohen, H. Schmidtmayerova, J. Dennis, L. Dubrovsky, B. Sherry, H. Wang, M. Bukrinsky, K.J. Tracey, The critical role of p38 MAP kinase in T cell HIV-1 replication, Mol. Med. 3 (1997) 339–346.
[13] M.R. Nonnemacher, T.H. Hogan, S. Quiterio, B. Wigdahl, A. Henderson, F.C. Krebs, Identification of binding sites for members of the CCAAT/enhancer binding protein transcription factor family in the simian immunodeficiency virus long terminal repeat, Biomed. Pharmacother. 57 (2003) 34–40.
[14] E.S. Lee, D. Sarma, H. Zhou, A.J. Henderson, CCAAT/enhancer binding proteins are not required for HIV-1 entry but regulate proviral transcription by recruiting coactivators to the long-terminal repeat in monocytic cells, Virology 299 (2002) 20–31.
[15] A.J. Henderson, X. Zou, K.L. Calame, C/EBP proteins activate transcription from the human immunodeficiency virus type 1 long terminal repeat in macrophages/monocytes, J. Virol. 69 (1995) 5337–5344.
[16] T.A. Kunkel, J.D. Roberts, R.A. Zakour, Rapid and efficient site-specific mutagenesis without phenotypic selection, Methods Enzymol. 154 (1987) 367–382.
[17] R. Horie, S. Aizawa, M. Nagai, K. Ito, M. Higashihara, T. Ishida, J. Inoue, T. Watanabe, A novel domain in the CD30 cytoplasmic tail mediates NFkappaB activation, Int. Immunol. 10 (1998) 203–210.
[18] R. Horie, M. Watanabe, T. Ishida, T. Koiwa, S. Aizawa, K. Itoh, M. Higashihara, M.E. Kadin, T. Watanabe, The NPM-ALK oncoprotein abrogates CD30 signaling and constitutive NF-kappaB activation in anaplastic large cell lymphoma, Cancer Cell 5 (2004) 353–364.
[19] T. Yuasa, S. Ohno, J.H. Kehrl, J.M. Kyriakis, Tumor necrosis factor signaling to stress-activated protein kinase (SAPK)/Jun NH2-terminal kinase (JNK) and p38. Germinal center kinase couples TRAF2 to mitogen-activated protein kinase/ERK kinase kinase 1 and SAPK while receptor interacting protein associates with a mitogen-activated protein kinase kinase kinase upstream of MKK6 and p38, J. Biol. Chem. 273 (1998) 22681–22692.
[20] J.A. Engelman, M.P. Lisanti, P.E. Scherer, Specific inhibitors of p38 mitogen-activated protein kinase block 3T3-L1 adipogenesis, J. Biol. Chem. 273 (1998) 32111–32120.
[21] J. Raingeaud, A.J. Whitmarsh, T. Barrett, B. Derijard, R.J. Davis, MKK3- and MKK6-regulated gene expression is mediated by the p38 mitogen-activated protein kinase signal transduction pathway, Mol. Cell. Biol. 16 (1996) 1247–1255.
[22] L. Shapiro, K.A. Heidenreich, M.K. Meintzer, C.A. Dinarello, Role of p38 mitogen-activated protein kinase in HIV type 1 production in vitro, Proc. Natl. Acad. Sci. U.S.A. 95 (1998) 7422–7426.
[23] X.Z. Wang, D. Ron, Stress-induced phosphorylation and activation of the transcription factor CHOP (GADD153) by p38 MAP kinase, Science 272 (1996) 1347–1349.
[24] T. Nakajima, S. Kinoshita, T. Sasagawa, K. Sasaki, M. Naruto, T. Kishimoto, S. Akira, Phosphorylation at threonine-235 by a ras-dependent mitogen-activated protein kinase cascade is essential for transcription factor NF-IL6, Proc. Natl. Acad. Sci. U.S.A. 90 (1993) 2207–2211.
[25] H.J. Tae, S. Zhang, K.H. Kim, cAMP activation of CAAT enhancer-binding protein-beta gene expression and promoter I of acetyl-CoA carboxylase, J. Biol. Chem. 270 (1995) 21487–21494.
[26] C. Trautwein, P. van der Geer, M. Karin, T. Hunter, M. Chojkier, Protein kinase A and C site-specific phosphorylations of LAP (NF-IL6) modulate its binding affinity to DNA recognition elements, J. Clin. Invest. 93 (1994) 2554–2561.
[27] S.M. Dunn, L.S. Coles, R.K. Lang, S. Gerondakis, M.A. Vadas, M.F. Shannon, Requirement for nuclear factor (NF)-kappa B p65 and NF-interleukin-6 binding elements in the tumor necrosis factor response region of the granulocyte colony-stimulating factor promoter, Blood 83 (1994) 2469–2479.
[28] S. Akira, T. Kishimoto, NF-IL6 and NF-kappa B in cytokine gene regulation. [Review] [215 refs], Adv. Immunol. 65 (1997) 1–46.
[29] G. Nabel, D. Baltimore, An inducible transcription factor activates expression of human immunodeficiency virus in T cells, Nature 326 (1987) 711–713.
[30] C. Trautwein, C. Caelles, P. van der Geer, T. Hunter, M. Karin, M. Chojkier, Transactivation by NF-IL6/LAP is enhanced by phosphorylation of its activation domain, Nature 364 (1993) 544–547.
[31] G.P. Rizzardi, A. Lazzarin, G. Pantaleo, Potential role of immune modulation in the effective long-term control of HIV-1 infection, J. Biol. Regul. Homeost. Agents 16 (2002) 83–90.

STEM CELLS AND DEVELOPMENT 17:67–80 (2008)

DOI: 10.1089/scd.2007.0077

Original Research Report

Identification of Transcripts Commonly Expressed in Both Hematopoietic and Germ-Line Stem Cells

TAKUO MIZUKAMI,[1] MADOKA KURAMITSU,[1] KAZUYA TAKIZAWA,[1] HARUKA MOMOSE,[1] ATSUKO MASUMI,[1] SEISHIRO NAITO,[1] ATSUSHI IWAMA,[2] TAKEHIKO OGAWA,[3] TOSHIAKI NOCE,[4] ISAO HAMAGUCHI,[1] and KAZUNARI YAMAGUCHI[1]

ABSTRACT

Germ-line stem cells (GSCs) constitute a stem cell population with remarkable stability and proliferative potential in vitro and are a useful model for studying the mechanism of self-renewal and "stemness" function of committed tissue stem cells. To identify GSC-specific genes, we performed subtractive hybridization using cDNA from GSCs, testis, and embryonic stem (ES) cells, and successfully identified 11 genes highly expressed in GSCs. Histological analysis confirmed expression of *Cryαb*, *Mcpt8*, *Cxcl5*, *Fth1*, *Ctla2α*, and *Spp1* in undifferentiated spermatogonia on the basement membrane area of the seminiferous epithelium of the testis, where the GSC niche is thought to be located. Among GSC-specific genes, quantitative PCR analysis showed seven genes—*Fth1*, *Cryαb*, *Spp1*, *Bcap31*, *Arhgap1*, *Ctla2α*, and *Serpina3g*—to be common transcripts highly expressed in hematopoietic stem cells (HSCs). Histological analysis confirmed that *Ctla2α*-, *Serpina3g*-, and *Spp1*-expressing cells were observed in the trabecular bone region of the bone marrow, where the HSC niche is located. Furthermore, histological analysis revealed that only *Spp1* was expressed in the hair follicle bulge in the area of the hair follicle stem cell niche. Thus, identifying stemness genes by comparative analysis to GSCs is a powerful tool with which to explore the fundamental commonalities of HSCs and other stem cell types.

INTRODUCTION

STEM CELLS ARE MAJOR TARGETS of regenerative medicine and gene therapy [1]. Among the various types of stem cells, hematopoietic stem cells (HSCs) have been studied as a useful model for stem cell research. HSCs are cells with self-renewal capacity and the ability to differentiate into all of the mature blood cell types [2]. HSCs require a specific microenvironment known as the HSC niche to maintain blood cell production throughout an organism's lifetime [3]. Recent studies demonstrate that the stem cell niche is in the vascular region [4] and the trabecular bone (TB) of the bone marrow [5]. Molecular analyses of the niche have shown that Notch [6], Wnt3a [7], Tie2 [8], Hoxb4 [9], and Bmi-1 [10] play crucial roles in HSC niche formation and self-renewal. In addition, several researchers reported genes commonly expressed by HSCs, embryonic stem (ES) cells, and neural stem cells (NSCs), using DNA microarray analysis [11–13]. However, much more information regarding common properties of stem cells is still required to elucidate the mechanisms of HSC niche formation and self-renewal.

[1]Department of Safety Research on Blood and Biological Products, National Institute of Infectious Diseases, Tokyo, Japan.
[2]Department of Cellular and Molecular Medicine, Graduate School of Medicine, Chiba University, Chiba, Japan.
[3]Department of Urology, Yokohama City University Graduate School of Medicine, Yokohama City University, Yokohama, Japan.
[4]Mitsubishi Kagaku Institute of Life Sciences, Tokyo, Japan.

Recently, various lines of stem cells have been characterized. Among them, we focused on the germ-line stem cell (GSC), a founder population for spermatogenesis [14]. In mammals, spermatogenesis takes places within the seminiferous epithelium of the testis and produces 100 million sperm each day in adult humans. Spermatogonia proliferate and differentiate into spermatocytes, and then differentiate into haploid spermatids and mature spermatozoa. It was proposed that spermatogonia were located on the basement membrane of the seminiferous tubules and that they can be divided into undifferentiated, differentiated, type B, and intermediate types based on their morphology [15]. Undifferentiated spermatogonia express the surface markers β1-integrin, α6-integrin, EpCAM, CD9, and Thy1 [16–19]. GSCs interact with Sertoli cells, which regulate and support the GSC niche via glial cell line-derived neurotrophic factor (GDNF) in the testis [20]. In vivo, GSCs constitute approximately 0.03% of the total testicular cells in the adult mouse testis [21] and divide slowly; however, in vitro, following GDNF treatment, the number of GSCs increases logarithmically without loss of capacity to produce mature spermatozoa when transplanted into recipient testis [22]. Over a 2-year period, the number of proliferating GSCs increases 10^{85}-fold without loss of their ability to produce mature spermatozoa and offspring [23]. It was reported that in vitro expansion of stem cells is possible only with ES cells [24] and embryonic germ cells [25], but these cell lines form teratomas when transplanted into the seminiferous epithelium and other tissues. Using GSCs, tumor formation was not observed in testis [26]. Thus, GSCs constitute a germ-line-committed stem cell population with remarkable stability and proliferative potential in vitro, and are a unique model for studying the self-renewal and expansion of committed tissue stem cells.

To define the molecular mechanisms governing common properties of tissue stem cells, we compared GSCs with HSCs, because both types of stem cells produce large numbers of differentiated cells (sperm and red blood cells, respectively) every day, throughout an organism's lifetime. Furthermore, it has been reported that mutations in the dominant-white spotting (*W*; c-kit) and stem cell factor (*Sl*; SCF) genes inhibit the proliferation, differentiation, and migration of various stem cell types, including HSCs [27] and GSCs [28]. Thus, HSCs and GSCs partially share common machinery for the regulation of stem cells.

Here, using subtractive screening, we identified 11 GSC-specific genes whose expression levels in GSCs were at least two-fold greater than those seen in testis. From an analysis of GSC-specific genes in HSCs, we identified seven genes that were common transcripts in both GSCs and HSCs. Furthermore, we found *Spp1* expression in hair follicle stem cells (HFSCs). Thus, identifying stemness genes by a comparative analysis of HSCs and GSCs is a powerful tool with which to explore the fundamental commonalities of HSCs and other stem cell types.

MATERIALS AND METHODS

Animals

To obtain fetal and neonatal testes and ovaries, 10 pregnant C57BL/6 mice were purchased from SLC (Shizuoka, Japan) and housed under constant temperature and light. Embryos and neonatal and postnatal mice were obtained at a variety of stages: 13.5 days post-coitus (dpc), 15.5 dpc, 17.5 dpc, newborn, 7 days after birth (dab), 14 dab, 28 dab, 8 weeks after birth, and 16 weeks after birth.

Histological preparation

Femur and tibias were harvested and fixed in Bouin's solution (Sigma-Aldrich Co., St. Louis, MO,) and supplemented with 0.01% glutaraldehyde at 4°C for 48 h for bone marrow non-decalcification in situ hybridization (ISH). For immunohistochemistry (IHC), femurs and tibias were fixed in 4% (wt/vol) paraformaldehyde in phosphate-buffered saline (PBS, pH 7.5). Other tissues, including testis, epidermal tissue, brain, and small intestine, were fixed with Bouin's solution at 4°C for 24 h for ISH, and fixed with 4% paraformaldehyde in PBS for IHC. After fixation, samples were dehydrated in a graded ethanol series and cleared in xylene. All tissues were embedded in paraffin. Eight micrometers (for ISH) or 4 μm (for IHC) semithin sections were cut using a carbon steel microtome blade (Feather Safety Razor Co., Osaka, Japan). Tissue sections were mounted on super-frosted glass slides coated with methylamino-silane (MAS) (Matsunami Glass, Osaka, Japan).

In situ hybridization

ISH of non-decalcified bone marrow and testis was carried using digoxygenin (DIG)-labeled RNA probes (0.6–0.8 kb). All probes were generated from corresponding coding sequences using a DIG RNA Labeling Kit SP6 / T7 (Roche Diagnostics, Tokyo, Japan). Target cDNA sequences were obtained by PCR amplification using specific primers (Table 1) and then subcloned into pGEM-T easy vector (Promega, Tokyo, Japan). For ISH with antisense and sense DIG-labeled cRNA probes, sections were prehybridized at 65°C in a humidified chamber for 1 h in prehybridization buffer containing 50 % formamide, 5× SSC, 5× Denhardt's solution, denatured salmon sperm DNA (Sigma-Aldrich, Tokyo, Japan), yeast tRNA (Roche Diagnostics), and 4% dextran sulfate. After prehybridization, 60 μl of hybridization mixture (prehybridization buffer plus DIG-labeled cRNA probe) was spotted on each slide, sealed under a coverslip, and incubated at 42°C for 24 h in a humidified chamber. After hybridization, coverslips were removed and slides were rinsed in 4× SSC at 37°C for 30 min. RNA in the tissue sections was digested with RNase A (20 μg/ml in 2× SSC) at 37°C for 60 min, and sections were rinsed in decreasing con-

TABLE 1. PRIMERS USED IN THIS STUDY

For GS verification

Gene	*Forward*	*Reverse*
β1-integrin	CACGGATGCTGGGTTTCAC	CCATCATTGGGTAAAACAATACCA
α6-integrin	GTTACCCTTTGGCCTTCTTTCTC	TGCATTTGGCGTCAGCAA
CD9	CGCAACTCCAGCTTGTACCA	GCAGGTATTTGATGCACTTGCT
EpCAM	CTTGGTATCCCTTTCGGCTTT	CGGATGTCGCGGACACA
PLZF	GCTGTGTGGGAAACGCTTTC	TGCGTGGACCTCCATGTG
c-kit	GGCCATGAACCTGGAAGAAG	ACTTTGGAAAGGTGCAAGAGTGT
Stra8	GAGTCCACCCCAGAAGAGATCCT	GTGGCAAACATAGCGCTGATG
Mvh	TTCCCATTGTATTAGCAGGACGAGAT	GAGCCAAAATAGGCAAGAGAAAAGC
Oct-4	TTCCCTCTGTTCCCGTCACT	TGGTGCCTCAGTTTGAATGC
Nanog	AGGCTGGACCGCTCAGT	AGTTATGGAGCGGAGCAGCAT

For HS verification

Gene	*Forward*	*Reverse*
CD34	GCATTGGTCACCTCTGGAGTTCT	AAGGGTCTTCACCCAGCCTTTC
Gata1	AGAAGCGAATGATTGTCAGCAAAC	GGTTCACCTGATGGAGCTTGAA
IL-7r	CATGTGCTATGGAAAAAAAGGATTAAAC	AGGAAACTTTCGGGATTGAAACTCA
SCL/tal-1	GGCCGAGCGCTGCTCTATA	CTTCACCCGGTTGTTGTTGGT
β-actin	CAGCCTTCCTTCTTGGGTATGG	CTGTGTTGGCATAGAGGTCTTTACG

For screening

Gene	*Forward*	*Reverse*
Acaa2	GCAGAGAACCTTGCTGCAAAATAC	AGCCAGCCTCGTTAGCAGCTT
Arbp	CTAGGACCCGAGAAGACCTCCTT	TCTTTATCAGCTGCACATCACTCAGA
Arhgap1	TTGCAGGCTCACGCTCTCA	GAGGATGACAGCGGGCAAGT
Asf1b	ATCCGTGTGGGCTACTATGTCAAC	CAAGATGTTCCGCTGTAGCTGAGA
Bcap31	CCAGCACCAAGAAAAAACTTGAGA	GTTCTTCTAGCAGGCGGTCATATTC
Ccl2	CACCAGCAAGATGATCCCAATG	GCTTGGTGACAAAAAACTACAGCTTCT
Cct8	CACGGGCACTGGCAGAAA	AGCAGGGACTTCAGCCTCGAT
Cox7c	GAGGGTCCGGGGAAGAATTT	AAAGAAAGGTGCGGCAAACC
Cryαb	TGACCTCTTCTCAACAGCCACTTC	CCTTCTCCAAACGCATCTCTGA
Ctla2α	ACGAAATTTGCAAAAGCCTACAATC	TGGTCTTGCCCTGCTCATAGTC
Cxcl5	TAGCTGAAGCTGCCCCTTCCT	GGGATTAATYTTTTTGGAGTTACGGTTAAG
Eno1	GTCCCTGCAGGCGTGTAAGC	ACCACCAGGTCTGCGATGAA
Fkbp6	AATATTCTGGATACCTGGAGCACATG	GCCCCAGAGTGTAATATCTTCTCCAA
FLG	TAAGGAGGAAGAAACACTGAGCAAAG	TGTCTTGGTCATCTGGATTCTTCAA
Fth1	CAAGAATGATCCCCACTTATGTGACT	TTCTGCCATGCCAGCTTCAG
High1	GCAGCGATTGTTGCCTATGG	ATGGCCCCCACAACAAAGC
Hspa8	GCCTATGGTGCAGCTGTCCAG	CATGACTCCGCCAGCAGTTTC
Ifnar2	ATGGTTTTCGTGAGCACTATCGTAAT	AAAAGTGGCGGAAGTTCAAGACA
Luc712	AACAACTAGGAGCTGAAGGAAATGTG	TAGAGTTCCGATAAACTTCCTCTGCTT
Map1lc3b	CCATGCCGTCCGAGAAGAC	CGCTCTATAATCACTGGGATCTTGGT
Mcpt8	CCAGAAGTGTCGCAGCATGTC	CGCCAGAGTCACCCTTACCAGTA
Mrps14	GCCAAAGGACCTTCAGGAAATG	GAGATGTCATAACACAGCGATTTCTG
Mt1	CCAACTGCTCCTGCTCCACC	ACAGCCCTGGGCACATTTG
Myo1c	TATGCCAACCTAACCGGAATCTC	ATCTCCCTTCTGCTTGTTGTCTTCA
Pps	ATGGTAACAACCCAAACCAGGTGTA	AGGAGCGAATCGGGATCTTG
Psmb6	CACTGCCAATGCTCTCGCTTT	CTGCCGCTCTACCCCTGACT

(continued)

TABLE 1. PRIMERS USED IN THIS STUDY (CONT'D)

Gene	*Forward*	*Reverse*
Ptma	CCGAGATCACCACCAAGGACTT	CTGCTCCCCATTTTCCTCATTT
Rpol-1	CACGTCCATAGTCCAGGATGAGAT	TGTTCCTTCCTCCTCTCCTTGGT
Rps19	CAGCCTTCCTCAAAAAGTCCG	GHTGGAAGCAGCTCGTGTGTAGAA
Saa3	CTGGGCTGCTAAAGTCATCAGTGA	GGCAAACTGGTCAGCTCTTGAG
Serpina3g	AGCTGGGCATCAGGGAAGTC	AGCCTTGTGGACCACCTGAGA
Spp1	ATTGGCAGTGATTTGCTTTTGC	TCTGGGTGCAGGCTGTAAAGCT
Ptges3	GATCGATTTTATGTTGTTTGCGAAA	GAAGTCCACACTGAGCCAATTAAGCT
Ywhae	GACATGCAGGGTGATGGTGAAG	GATGGTTTCTCTTGTTGGCTTTTATTT

For in situ hybridization

Gene	*Forward*	*Reverse*
CD34	GACAACATGTGGTGGCTGAC	GTCAGAGGAAGGGGGAAGTC
Tie2	CCCTCCTCAACCAGAAAACA	GCACTCTGCTCTTACCCAGG
Bmi-1	GGAGAGACAATGGGGAGGTT	GCATCACAGTCATTGCTGCT
SCL/tal-1	TGGGACAATGTGGTCAGCTA	CTGTGCCCTTGGTTTTTGTT
Ctla2α	CCTCTGCTTGGGAATGATGT	TACACAAAGCAGGTGCTGGA
Luc712	ACTTCGTGTCTGCGAGGTCT	AAGCTGCTGCTGTTTGGAAT
Spp1	TGGTGATCTAGTGGTGCCAA	TTGTCCTTGTGGCTGTGAAA
Fth1	AACAGTGCTTGAACGGAACC	AAAAGATGAAGGCAGCCTGA

centrations of SSC (2× SSC and then 0.1× SSC) for 60 min at 50°C. Hybridized DIG-labeled cRNA was detected using an alkaline phosphatase-labeled anti-DIG antibody (Roche Diagnostics). Sections were stained using a BCIP/NBT detection kit (Nakarai, Kyoto, Japan) and mounted with Gel Mount (Biomeda Corp, Foster City, CA).

Double ISH was performed by combining *Spp1* DIG-cRNA and *Tie2* biotin cRNA probes [29]. After prehybridization, sections were hybridized with prehybridization buffer plus DIG-labeled *Spp1* and biotin-labeled *Tie2* probes at 50°C for 36 h. Sections were then rinsed and incubated with RNase A at 37°C for 1 h. cRNA probes were detected using the tyramide signal amplification (TSA) fluorescein system (Perkin Elmer, Kanagawa, Japan). DIG-labeled cRNA for *Spp1* was first detected using an anti-DIG POD antibody (Roche Diagnostics) conjugated to fluorescein. After inactivation of peroxidase with 3% H_2O_2, biotin-labeled cRNA for *Tie2* was detected using an anti-biotin POD antibody (Roche Diagnostics) conjugated to Cy3. After detection, images of histological sections were obtained using an Eclipse E1000 fluorescence microscope equipped with a digital DXM1200 camera (Nikon, Tokyo, Japan). Digital images were analyzed with Photoshop 7 (Adobe systems Inc., San Jose, CA) and NIH-image 1.62 (Scion Image Co, Frederick, MD).

Immunohistochemistry

A rabbit anti-mouse osteopontin antibody (LB4225; LSL/Cosmo Bio, Tokyo, Japan) and an anti-mouse Serpina3g (ab36772; Abcam, Koto-ku, Japan) monoclonal antibody were used in this study. Staining was carried out as previously described [30]. Briefly, after blocking with 3% bovine serum albumin (BSA) in PBS, sections (4 μm thick) were incubated with anti-osteopontin antibody (diluted 1:400) and anti-Serpina3g antibody (diluted 1:50) at 4°C overnight. Signals were detected using a VECTASTAIN ABC Kit (Vector Laboratory Inc., Burlingame, CA), and nuclei were stained with Hematoxylin.

Cell preparation

Germ-line stem cell and ES cell. GSCs established previously [31] were cultured in Stem Pro-34 SFM medium (Invitrogen, Tokyo, Japan) containing Stem Pro supplement, insulin (25 μg/ml), transferrin (100 μg/ml), putrescine (60 μM), sodium selenite (30 nM), D-(+)-glucose (6 mg/ml), pyruvic ascid (30 μg/ml), DL-lactic acid (1 μl/ml), bovine serum albumin (5 mg/ml), L-glutamine (2 mM), 2-mercaptoethanol (5×10^{-5} M), minimal essential medium vitamin solution (Invitrogen), MEM nonessential amino acid solution, ascorbic acid (10^{-4} M), *d*-biotin (10 μg/ml), mouse epidermal growth factor (EGF; 20 ng/ml, BD science, Tokyo, Japan), human basic fibroblast growth factor (bFGF; 10 ng/ml, BD Science), ESGRO (10^3 U/ml murine leukemia inhibitory factor, LIF; Invitrogen), recombinant rat glial cell line-derived neutrophic factor (GDNF; R&D systems, Minneapolis, MN), and 1% fetal bovine serum (FBS). Cells were maintained at 37° in an atmosphere of 5% carbon dioxide in air.

ES cells. E14TG2a ES (XY) cells [32] were also maintained in standard ES cell culture conditions.

Bone marrow cells. Bone marrow cells were harvested from the femurs and tibias of C57BL/6 mice. After separation of red

blood cells using Lymphoprep (Invitrogen); mononuclear cells were stained with biotinylated antibodies to various lineage markers. Lineage-positive (Lin^+) cells were depleted, with streptavidin-conjugated magnetic particles using a MACS CS column (Miltenyi Biotec K.K., Toshima-ku, Japan). Lineage-depleted cells were collected and incubated with anti-Sca-1 (conjugated to phycoerythrin, PE), anti-c-kit (conjugated to allophycocyanin, APC), and anti-CD34 (conjugated to fluorescein, FITC) (eBioscience Inc., San Diego, CA). Stained cells were fractionated by fluorescence-activated cell sorting (FACS) JSAN (Bay Bioscience Co., Kobe, Japan).

Subtraction based on selective-suppression PCR

Poly(A)$^+$ RNAs from GSCs, BM cells, and ES cells were extracted using a Micro-FastTrack™ 2.0 Kit (Invitrogen), and cDNAs were prepared using a PCR Select cDNA Subtraction Kit (BD Science), according to the manufacturer's instructions. Suppression-subtractive hybridization was performed according to Menke et al. [33]. Briefly, after digestion with *Rsa* I and *Alu* I, tester cDNAs (from GSCs) were ligated separately with two different adaptors (A and B) and amplified by PCR using biotinylated and nonbiotinylated primers corresponding to the adapter sequences. The driver cDNA (from testis and ESCs) pool was generated using a third adaptor (C) and corresponding primers. Biotinylated and nonbiotinylated tester cDNAs (bio-A+B) were mixed with excess driver cDNA and hybridized for 4 days. The resulting subtracted cDNAs were purified using streptavidin-bound magnetic particles (Roche Diagnostics). Combining these with other subtraction products using another set of tester cDNAs (A+bio-B), we performed a series of three subtractive procedures. The resulting subtracted cDNA fragments were cloned into the pGEM-T Easy vector (Promega), sequenced, and compared with the National Center for Biotechnology Information (NCBI) database using BLAST.

Quantitative analysis of gene expression

Real-time PCR was carried out on single-stranded cDNAs prepared using the Super Script First-Strand Synthesis System (Invitrogen) and an oligo(dT) primer. PCR reactions were performed using SYBR PreMix ExTaq™ (TAKARA Shuzo, Kyoto, Japan) and a Light Cycler (Roche Diagnostics). The primer pairs used for GSC verification are shown in Table 1. We used β-actin as an internal control. Real-time PCR was carried out for 40 cycles of 94.0°C for 1 min and 60°C for 25 s (two-step). Amplification of predicted fragments was confirmed by melt-curve analysis and gel electrophoresis. To determine the relative amounts of products, we used the comparative CT (threshold cycle) method, according to the manufacturer's instructions (Roche Diagnostics). Expression is reported relative to mouse β-actin.

RESULTS

Isolation of mouse germ-line stem cells

To isolate mouse GSCs, testicular germ cells from DBA/S mice were cultured in the presence of cytokine cocktail containing EGF, bFGF, LIF, and GDNF [21–22]. After three passages, GSCs were plated on mouse embryonic fibroblast (MEF) feeder layer. Floating GSCs were passaged four times. They formed colonies, which were contained 10–50 round GSCs. Each GSC colony

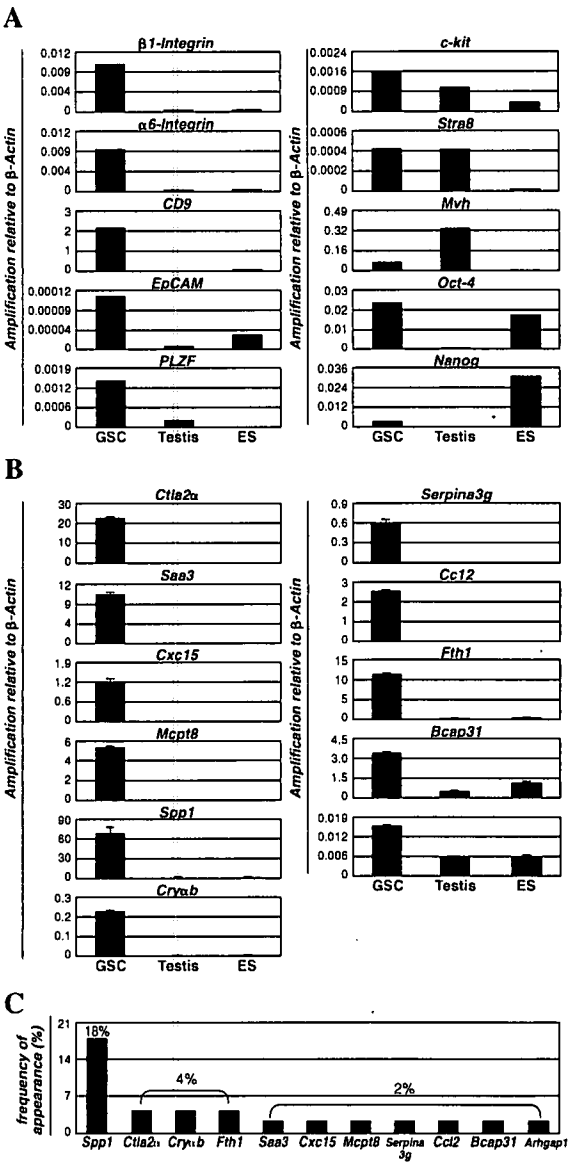

FIG. 1. Quantitative real-time PCR of GSCs, ES cells, and testis. (**A**) Expression of *β1-integrin, α6-integrin, CD9, EpCAM, Plzf, c-kit, Stra8, Mvh, Oct-4,* and *Nanog* in 6 month-cultured GSCs. (**B**) The relative amounts of the 11 GSC-specific genes identified in this study were analyzed in GSCs, ES cells, and testis. Expression is relative to mouse *β-actin.* Means ± SEM for two experiments are shown. (**C**) Frequency of appearance of 11 GSC-specific genes within 56 clones we picked.

was positive for the spermatogonial marker TRA98 (data not shown). For RNA purification, 1×10^6 GSCs were used in this study. To confirm the character of GSCs, we performed real-time PCR analysis with specific primers (Table 1). Six-month cultured GSCs specifically expressed several undifferentiated spermatogonial surface markers, including *β1-integrin*, *α6-integrin*, *CD9*, *Ep-CAM*, and *Plzf* (Fig. 1A). The expression of the differentiated spermatogonia marker *c-kit* and *Stra8* was detected in GSCs and testis. The expression level of the germ cell marker *Mvh* was not prominent in GSCs compared to those in testis. Although GSCs expressed the ES cell marker *Oct-4*, they did not express another ESC-specific marker, *Nanog*. These data suggest that 6-month cultured GSCs constitute a stem cell population and with the potential of undifferentiated spermatogonia in vitro.

Subtractive suppression hybridization screening for GSC-specific genes

To identify GSC-specific genes, we performed a screen in which cDNAs from testis and ES cells were subtracted from cDNA of GSCs. In this screen, we picked 56 clones and identified 34 genes (Table 1). The expression levels of individual genes were quantified by real-time PCR, which confirmed high expression of the screened genes in GSCs compared with testis (Table 2 and Fig. 1B). Specifically, we identified 11 new genes (*Ctla2α*, *Saa3*, *Cxcl5*, *Mcpt8*, *Spp1*, *Cryαb*, *Serpina3g*, *Ccl2*, *Fth1*, *Bcap31*, and *Arhgap1*) whose expression levels in GSCs were at least two-fold greater than those seen in testis. Among them, eight genes, *Ctla2α*, *Saa3*, *Cxcl5*, *Mcpt8*, *Spp1*, *Cryαb*, *Serpina3g*, and *Ccl2* were expressed at levels more than 10 times as high as those seen in testis. The frequency of appearance of GSC-specific genes in the 56 clones we examined is shown in Fig. 1C. Within the 56 clones, *Spp1* appears nine times (18%); *Ctla2α*, *Cryαb*, and *Fth1* appear two times each (4%), and the other seven genes appear only once each (2%). These data suggest that *Spp1* is common in the subtracted cDNA of GSCs. Thus, we focused on *Spp1* expression in the testis. Although our screened GSC-specific genes were described and predicted in the National Center for Biotechnology Information (NCBI) Entrez gene information (gene ontology), their functions in GSCs and other stem cell lines are not clear at present.

Expression patterns of GSC-specific genes in the testis

As a result of subtractive suppression hybridization screening and quantitative gene expression analysis, we identified 11 genes that are highly expressed in GSCs. Among them, *Spp1* appeared frequently in the clones we picked, and is highly expressed in GSCs. These data suggest that *Spp1* has an important role in the regulation of GSCs. To confirm *Spp1* expression in the testis, we performed ISH and IHC for *Spp1*. ISH analysis showed expression of *Spp1* in the spermatogonia on the basal membrane throughout the cycle of the seminiferous epithelium (Fig. 2A). Intense expression of *Spp1* in spermatogonia was observed in the cycle of the seminiferous epithelium at stages VII and VIII (Fig. 2B). IHC of Spp1 confirmed the ISH analysis, showing that Spp1 protein is present in the spermatogonia at stages VII and VIII (Fig. 2C,D). To determine the role of *Spp1* in GSCs, we performed IHC for the Spp1 protein in the developing mouse testis and ovary. Spp1 protein was not observed in the primordial

TABLE 2. RELATIVE AMOUNTS OF 11 TRANSCRIPTS IN GSCS, HSCS, AND ES CELLS AS DETERMINED BY QUANTITATIVE REAL-TIME PCT

Symbol	*Full name*	*GSCs*	*ES cells*	*Testis*
Ctla2α[a]	Cytotoxic T lymphocyte associated protein 2 alpha	777.84	0.00	1
Saa3	Serum amyloid A3	642.11	0.17	1
Cxcl5	Chemokine(c-x-c motif) ligand 5	580.04	0.02	1
Mcpt8	Mast cell protease	422.65	0.00	1
Spp1[a]	Secreted Phosphoprotein-1/Osteopontin	356.07	12.27	1
Cryαb[a]	Crystallin αB (Small heat shock protein)	318.10	14.16	1
Serpina3g[a]	Serine or Cysteine proteinase inhibitor, clade A, member 3G	152.22	0.00	1
Ccl2	Chemokine (C-C motif) ligand 2	146.69	0.02	1
Fth1[a]	Ferritin Heavy Chain 1	13.58	0.52	1
Bcap31[a]	B-cell receptor-associated protein 31	7.43	2.61	1
Arhgap1[a]	Rho GTPase activating protein 1	2.68	1.07	1

Data show the expression level relative to that in the testis.
[a]Gene expression was detected in HSCs.

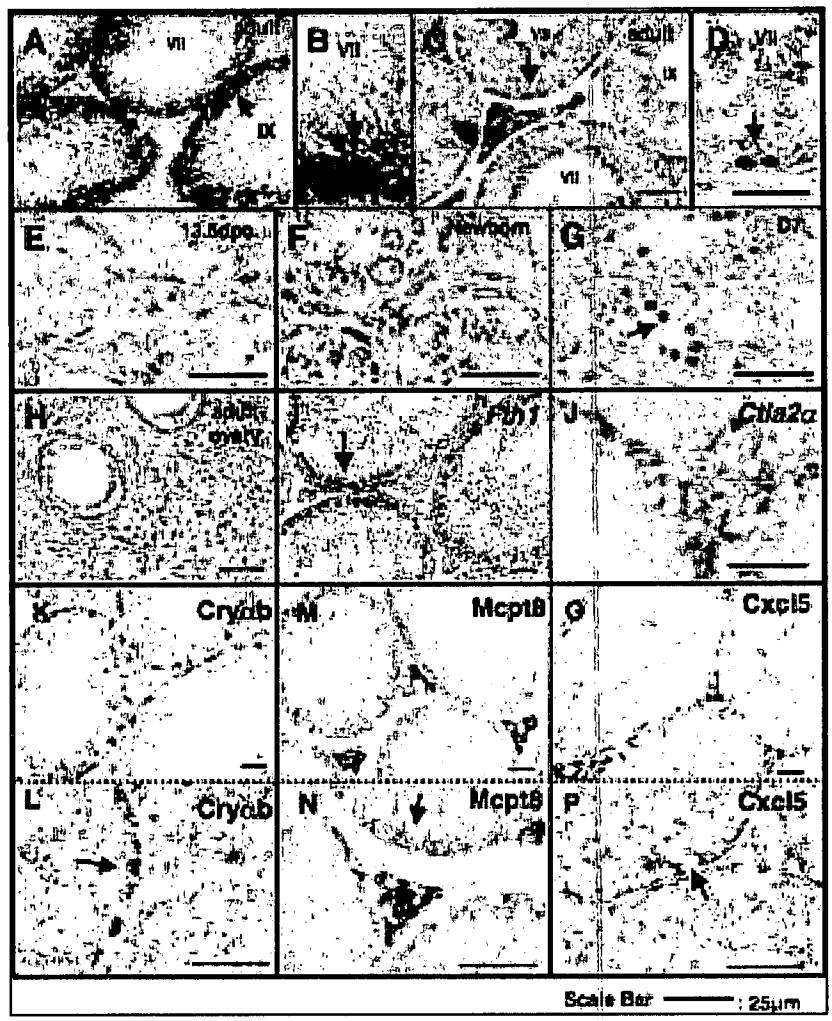

FIG. 2. Expression patterns of *Spp1*, *Fth1*, *Ctla2α*, *Cryαb*, *Mcpt8*, and *Cxcl5* in the testis. (**A**) In the adult testis, spermatogonia weakly express *Spp1* mRNA throughout the stages, as shown by ISH. Intense expression (arrow) was observed at cycles of the seminiferous epithelium in stages VII and VIII. (**B**) High magnification of intense expression of *Spp1* in testis. (**C**) Spp1 protein was also detected in spermatogonia (arrow) at stages VII and VIII by IHC. (**D**) High magnification of Spp1 protein in testis (arrow). Spp1 protein was not detected in the fetal testis (13.5 dpc) (**E**) or in the newborn testis (**F**). (**G**) Spp1 protein was first observed in the testis 7 days after birth (arrow). (**H**) No specific expression was observed in the fetal and adult ovary. (**I**) ISH of *Fth1* in adult testis. The expression of *Fth1* mRNA is presented in undifferentiated (arrow) and differentiated spermatogonia and early spermatocytes. (**J**) The expression pattern of *Ctla2α* mRNA detected by ISH is presented in undifferentiated spermatogonia. (**K,L**) IHC of Cryαb in the adult testis. Arrow indicates Cryαb$^+$ undifferentiated spermatogonia. (**M,N**) IHC of Mcpt8 in the adult testis. Mcpt8 protein is presented in spermatogonia and Leydig cells. Arrow indicates Mcpt8$^+$ spermatogonia. (**O,P**) IHC of Cxcl5 in adult testis. Cxcl5 protein is presented in spermatogonia. Arrow indicates Cxcl5$^+$ undifferentiated spermatogonia. Bar, 25μm. Roman numerals indicate the stage of the seminiferous tubule.

germ cells (PGCs) obtained from 13.5 (Fig. 2E), 15.5, and 17.5 (data not shown) dpc mice, indicating that PGCs and early gonocytes do not express *Spp1*. In the newborn testis, gonocytes began to arise in the seminiferous tubule and type A_{single} spermatogonia first appear at day 6 [34]. Spp1 protein was not detected in gonocytes in the newborn testis (Fig. 2F). Seven days after birth, Spp1 protein was first observed in gonocytes located both in the lumen of the seminiferous epithelium and on the basement membrane of the seminiferous epithelium, indicating that Spp1 is abundantly expressed in type A_{single} spermatogonia (Fig. 2G). After the first wave of spermatogenesis, Spp1 protein was seen in spermatogonia at stages VII and VIII (Fig. 2C). *Spp1* expression and Spp1

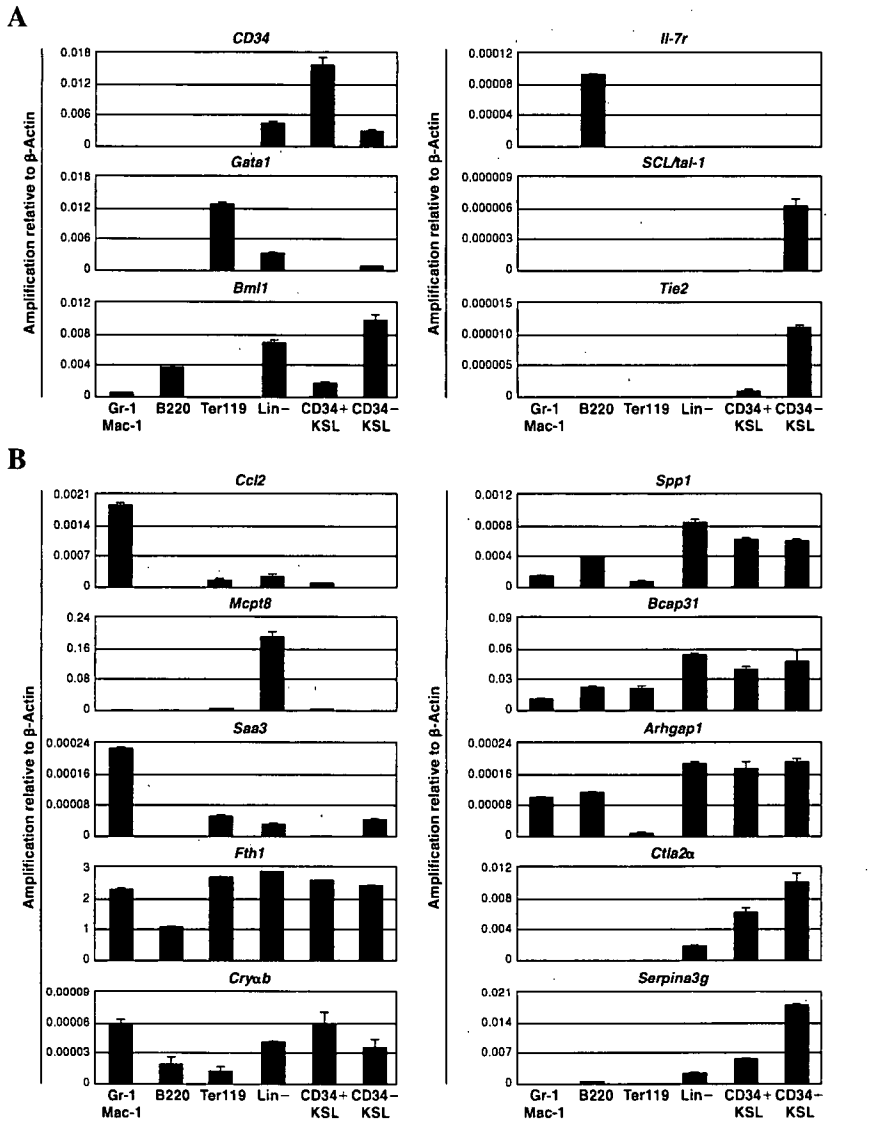

FIG. 3. Quantitative real-time PCR in the bone marrow. (**A**) Expression of *CD34, Il-7r, Gata-1, SCL/tal-1, Bmi-1,* and *Tie2* in the bone marrow. (**B**) Expression of *Ccl2* and *Saa3* were detected in Gr-1/Mac-1$^+$ cell fraction. Expression of *Mcpt8* was detected in the Lin$^-$ cell fraction. *Fth1* expression was detected in KSL cells (kit$^+$/Sca-1$^+$/Lin$^-$) and other cell lineages. *Cryαb* expression was detected in KSL and Gr-1/Mac-1 fractions. *Spp1, Bcap31,* and *Arhgap1* were detected in the KSL. The expression levels of *Ctla2α* and *Serpina3g* in CD34$^-$ KSL cells was higher than that in CD34$^+$ KSL cells.

FIG. 4. Expression patterns of *Spp1, Ctla2α,* and *Serpina3g* in bone marrow. (**A**) *CD34*-expressing cells (arrow) were widely distributed in the bone marrow. (**B**) *Bmi-1*-expressing cells (arrow) were located at the endosteal region of TB. (**C**) *SCL/tal-1*-expressing cells (arrow) were located at the endosteal region (arrow) of TB. (**D**) *Tie2*-expressing cells (arrow) were located at the endosteal region of TB. (**E**) *Spp1*-expressing cells were detected at the TB (arrow) by ISH. (**F**) High magnification of *Spp1* expression in BM. *Spp1* expression was detected both in HSCs (arrow) and osteoblasts (arrowhead). (**G–I**) Double ISH of *Spp1* and *Tie2* in the TB. *Tie2* and *Spp1* are partially co-expressed (arrow). The boxed area shows a high magnification of double ISH of Spp1 and Tie2. (**J**) Ctla2α-expressing cells (arrow) were observed only in the TB. (**K**) At the endosteal region of TB, some Ctla2α-expressing cells were attached to osteoblasts. (**L,M**) Using IHC, Serpina3g-expressing cells (arrow) were observed at the TB region. (Dotted line) Endosteal region of the TB. Bar, 25μm.

FIG. 5. Expression pattern of *Spp1* in the hair follicle bulge. (**A**) Hematoxylin & Eosin staining of a hair follicle. (**B**) A few *Spp1*-expressing cells (arrow) are observed at the bulge region by ISH. (**C**) The HFSC marker *CD34* (arrow) was detected at the same region as *Spp1* by ISH. (Dotted line) Hair follicle. Bar, 25μm.

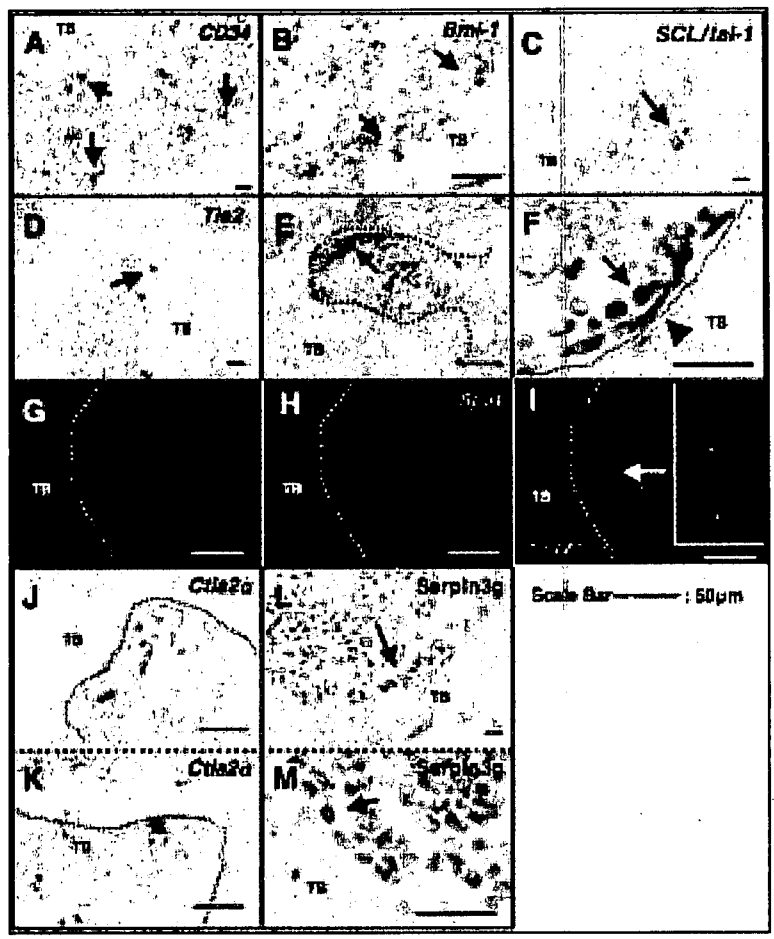
A
CD34
TB
B
Bmi-1
TB
C
SCL/tal-1
TB
D
Tie2
TB
E
TB
F
TB
G
TB
H
TB
I
TB
J
Ctla2a
TB
L
Serpin3g
TB
Scale Bar——— : 50μm
K
Ctla2a
TB
M
TB

FIG. 4.

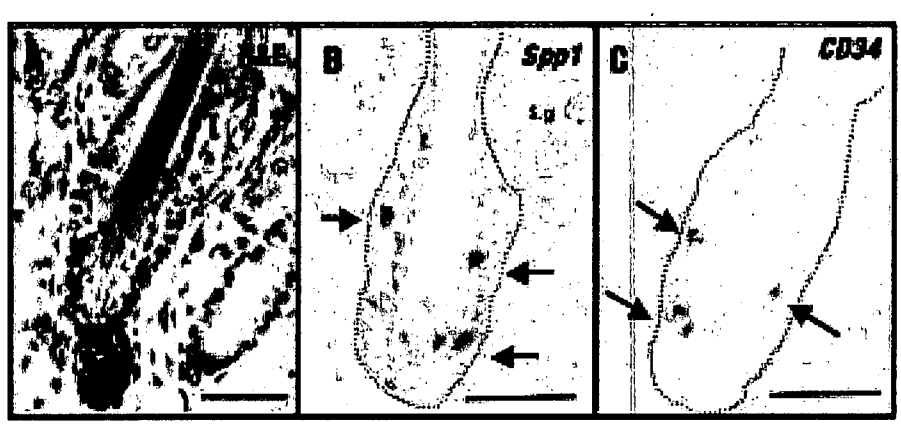
B
Spp1
C
CD34

FIG. 5.

protein were not seen in female germ cells in the fetal, neonatal (data not shown) and adult ovary (Fig. 2H). These data suggest that Spp1 is involved in spermatogonial stem cell fate determination from gonocytes.

To confirm the localization of other screened GSCs-specific genes, we performed ISH for *Fth1* and *Ctla2α*, and IHC for Cryαb, Mcpt8, and Cxcl5. Using ISH, *Fth1* mRNA was detected in the spermatogonia on the basal membrane of the seminiferous epithelium and spermatocyte (Fig. 2I). *Ctla2α* mRNA was detected in the undifferentiated spermatogonia on the basal membrane of the seminiferous epithelium (Fig. 2J). Cryαb protein was detected in undifferentiated spermatogonia on the basal membrane of the seminiferous epithelium (Fig. 2K,L). Cryαb-positive spermatogonia were present throughout the seminiferous epithelium cycle, indicating that Cryαb is abundantly expressed in undifferentiated spermatogonia (GSCs). Mcpt8 protein was detected in the spermatogonia on the basal membrane of the seminiferous epithelium and Leydig cells (Fig. 2M,N). Cxcl5 protein was detected in the spermatogonia on the basal membrane of the seminiferous epithelium and Leydig cells (Fig. 2O,P). Immunoreactivity with the anti-Cxcl5 antibody was seen only in the cytoplasm of spermatogonia and was highly accumulated at the basement membrane area, indicating that *Cxcl5* is abundantly expressed in both undifferentiated and differentiated spermatogonia.

Quantitative gene expression analysis of various cell types in the bone marrow

To identify genes expressed in both HSCs and GSCs, we performed real-time PCR and quantified the expression levels of 11 GSC-specific genes in fractionated BM cells (Fig. 3). Before analyzing these genes, we checked the expression levels of *CD34, IL-7r, Gata-1, SCL/tal-1, Tie2*, and *Bmi-1* in each cDNA panel from fractionated BM. *CD34, IL-7r, Gata-1*, and *SCL/tal-1* were highly expressed in the $CD34^+$ KSL cell fraction, the $B220^+$ cell fraction, the $Ter119^+$ cell fraction, and the $CD34^-$ KSL cell fraction, respectively (Fig. 3A). The expression levels of genes related to self-renewal and the HSCs niche were higher in the $CD34^-$ KSL cell fraction than in the $CD34^+$ KSL fraction (Fig. 3A). These included *Hoxb4* (three-fold increase; data not shown), *Bmi-1* (five-fold increase), and *Tie2* (14-fold increase). These results suggest that the sorted fractions reflect each cell type found in bone marrow. Thus, we determine that the Gr-1/Mac-1^+ cell fraction contains granulocyte and macrophage progenitors, the $B220^+$ cell fraction contains B cell progenitors, the $Ter119^+$ cell fraction contains erythroid progenitors, the Lineage-negative (Lin^-) cell fraction contains other cell types in bone marrow, the $CD34^+$ KSL ($CD34^+$/c-kit^+/Sca-1^+/Lin^-) cell fraction contains ST-HSCs, and the CD34-KSL ($CD34^-$/ c-kit+ / Sca-1^+/ Lin^-) cell fraction contains LT-HSCs.

When we analyzed the expression level of 11 GSC-specific genes in sorted bone marrow cell fractions by quantitative real-time PCR, we found that seven genes, *Fth1, Cryαb, Spp1, Bcap31, Arhgap1, Ctla2α*, and *Serpina3g* were expressed in both LT-HSCs plus ST-HSCs (Fig. 3B). *Ccl2* and *Saa3* were expressed in the Gr-1/Mac-1 fraction and *Mcpt8* was expressed in the Lin^- fraction. *Cxcl5* expression was not detected in any fraction. Although *Fth1* and *Cryαb* were expressed in LT-HSCs as well as ST-HSCs, Fth1 was expressed in other fractions and *Cryαb* was expressed in the Gr-1/Mac-1 fraction. Among the seven genes, *Spp1, Bcap31, Arhgap1, Ctla2α*, and *Serpina3g* were highly expressed in ST-HSCs as well as LT-HSCs. The expression levels of *Ctla2α* (1.58-fold) and *Serpina3g* (3.04-fold) in LT-HSCs were higher than those in ST-HCS.

Spp1, Ctla2α, *and* Serpina3g *expression in the bone marrow*

As a result of quantitative gene expression analysis, we identified seven genes that are highly expressed in both GSCs and HSCs. Among them, *Spp1* appeared frequently in the clones we picked, and is highly expressed in GSCs and ST- and LT-HSCs. These data suggest that Spp1 has important roles in the regulation of stem cells. To confirm expression patterns in the bone marrow, we performed histological analyses using specific *Spp1* probes. It is proposed that HSCs require a specific microenvironment known as the HSC niche, located in the vascular region [4] and the TB of the bone marrow [5], as the genes encoding CD34, Tie2 [8], SCL/tal-1 [35], and Bmi-1 [10] are reported to be crucial for both HSC self-renewal and niche maintenance. Before analyzing *Spp1* expression in the BM, we confirmed the expression patterns of these genes as a niche indicator in the bone marrow by ISH. As shown in Fig. 4A, some *CD34*-expressing cells were located at the endosteal region of the TB, where the HSC niche is located, whereas almost all *CD34*-expressing cells were widely distributed in the bone marrow. On the other hand, *Bmi-1-, SCL/tal-1-*, and *Tie2*-expressing cells were observed at the endosteal region of the TB (Fig. 4B, C and D). These data support the osteoblastic zone as one of the possible candidates of HSC niche.

It was reported that Spp1 functions in osteoblast differentiation and that it is present in osteoblasts in the bone marrow [36]. As shown in Fig. 4E, expression of Spp1 was mainly observed in osteoblasts of the TB. *Spp1* expression was also detected in HSCs located at the TB. Some *Spp1*-expressing HSCs were attached to *Spp1*-expressing osteoblast [Fig. 5F]. These data suggest that Spp1 has multiple functions both in HSCs and osteoblasts

as a niche regulator. To characterize *Spp1*-expressing HSCs in the bone marrow, we performed double ISH for *Spp1* and *Tie2*. Whereas *Tie2- and Spp1*-expressing cells were mainly observed at the TB (Fig. 4G,H), double-positive cells expressing both *Tie2* and *Spp1* were only seen at the TB (Fig. 4I). These data suggest that some *Spp1*-expressing cell express *Tie2* in the TB and function to regulate HSCs.

Among our identified genes, expression of *Ctla2α* and *Serpina3g* was detected in LT-HSCs. Thus, we hypothesized that these genes could act as HSC regulators and as indicators of the HSC niche. To analyze the expression patterns of our screened genes in the BM, we performed ISH with a *Ctla2α*-specific probe and IHC with an anti-Serpina3g antibody. In the bone marrow, *Ctla2α*- and *Serpina3g*-expressing cells were present mainly at the endosteal region of the TB. *Ctla2α*-expressing cells were mainly present in the TB (Fig. 4J,K). Serpina3g-expressing cells were mainly present in the TB (Fig. 4L,M). These data suggest that both *Ctla2α* and *Serpina3g* are useful markers and niche indicators of the HSC niche.

Spp1 *is expressed in HFSCs*

Spp1 is highly expressed in both HSCs and GSCs. These data suggest that Spp1 has a common role in the regulation of various types of tissue-committed stem cells. It was reported that tissue stem cells reside within a specific microenvironment niche [37]. To confirm a common role of *Spp1* in other stem cell niches, we performed ISH for *Spp1* in the mouse intestinal crypt (containing intestinal epithelial precursors), the gastric isthmus (containing gastric epithelial precursors), the skin (containing interfollicular epithelial stem cells), the hair follicle bulge (containing epithelial stem cells; HFSCs), the subventricular zone of lateral ventricle, and the subgranular zone of hippocampus (containing NSCs). ISH for *Spp1* in various tissue stem cell niches showed that *Spp1* expression was robust in a few cells at the hair follicle bulge in hair follicles and epidermal tissue (Fig. 5A,B). *Spp1*-expressing cells were coincident with CD34-expressing cells, which are located in the hair follicle bulge (Fig. 5C). Together, these data indicate that *Spp1* is expressed in HSCs, GSCs, and HFSCs, located in a region associated with stem cell activity, suggesting that *Spp1* may regulate stemness in the various tissue stem cell systems (Fig. 6).

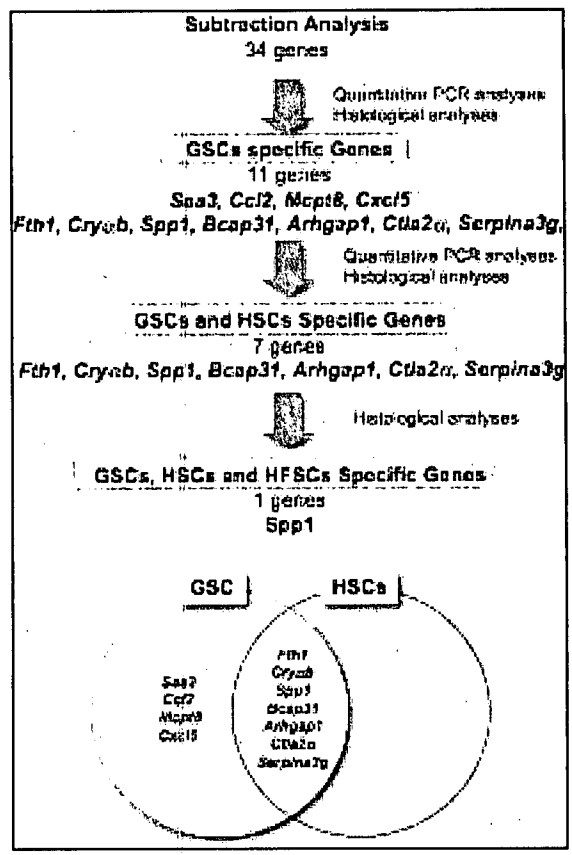

FIG. 6. Summary of our screening. Venn diagram of gene symbols in each stem cell line and their overlaps.

DISCUSSION

In this study, we performed subtractive hybridization using cDNA from GSCs, testis and ESCs, and successfully identified 11 genes that are highly expressed in GSCs (Table 2). Histological analysis confirmed the expression of *Cryab, Mcpt8, Cxcl5, Fth1, Ctla2α*, and *Spp1* in the undifferentiated spermatogonia on the basement membrane area of the seminiferous epithelium of the testis, where the GSC niche is thought to be located. Other genes were not tested in this study. The GSC-specific genes we identified in this study showed various expression patterns in the testis (Figs. 1 and 2) and contribute to our understanding of the self-renewal mechanism and differentiation of spermatogonia.

Cryαb (αB-Crystallin), a member of the small heat shock protein family, possesses chaperone-like function. Cryαb is expressed in lens [38] and other tissues [39]. Expression of *Cryab* is induced by thermal, osmotic, and oxidative insults, indicating that *Cryab* may have a protective role against apoptosis [40]. Although heat stress can disrupt germ cells in the testis [14], undifferentiated spermatogonia are resistant to short-term heat stress [41]. In our research, we clearly showed that *Cryab* is present in GSCs and HSCs, suggesting that *Cryab* could be a possible candidate gene that protects stem cells from various stresses.

Among the GSC-specific genes, *Spp1* appeared frequently among the 56 clones we picked following subtracted cDNA experiments, and was highly expressed in GSCs. Spp1 is a phosphorylated glycoprotein produced by many cell types, and it functions in many physiological processes [42]. Until now, however, the function of Spp1 in GSCs has not been clear. It was reported that spermatogonia are divided into undifferentiated spermatogonia and differentiated spermatogonia. Undifferentiated spermatogonia proliferate and form $A_{aligned}$ spermatogonia at epithelial stages VII–VIII [43]. Our expression analysis revealed that *Spp1* mRNA and protein are present in undifferentiated spermatogonia throughout the cycle of the seminiferous epithelium, but high expression of *Spp1* mRNA and Spp1 protein were observed only at stages VII and VIII. These data suggest that Spp1 could have function in the self-renewal of undifferentiated spermatogonia. It was reported that GSCs first arise from gonocytes, which are derived from PGCs in the embryonic gonad [44]. Our developmental study clearly showed that *Spp1* expression was up-regulated in early GSCs at day 7, when gonocytes differentiate into GSCs. Further analyses are required to determine the function of Spp1 in GSCs.

Using DNA microarrays and proteomics analysis, several researchers have reported genes that are highly expressed in GSCs, distinct from those expressed in ES cells [45] and multipotent GSCs (mGSCs) and ES cells [46]. None of their identified genes in GSCs were included in our analyses. These authors focused on stemness genes in GSCs associated with stem cell mutipotency by comparing GSCs with ES cells and mGSCs. It was proposed that GSCs express some ES cell marker [23]. However, these ES cell-specific genes were not identified in our screening. Thus, we hypothesized that as a result of subtraction of ES cell cDNA of from GSC cDNA, we could successfully deplete genes associated with stem cell multipotency and identify genes related to tissue-committed GSCs.

As shown in Fig. 6, we identified seven genes in common between GSCs and HSCs from 34 candidate genes. Several researchers have reported a molecular signature of stemness using DNA microarray analysis of ES cells, HSCs and NSCs [11–13]. Ramalho-Santos et al. identified 230 genes commonly expressed in ES cells, NSCs, and HSCs [11]. Ivanova et al. reported 283 stem cell-related genes commonly expressed in ES cells, HSCs, and NSCs [12]. Despite the massive amount of genetic information concerning stemness reported by these two groups, the genes identified in this study as commonly expressed in GSCs and HSCs were not included in their data. These data suggest that GSCs have a unique set of stemness genes, and comparison screening between GSCs and HSCs enables the identification of unique gene sets.

Among seven common genes, we successfully identified three promising genes, *Spp1*, *Ctla2α*, and *Serpina3g*. *Spp1* mRNA was detected in some osteoblasts and HSCs at the TB in the bone marrow. Spp1 produced by osteoblasts reportedly functions as a negative regulator of niche size by suppressing the expression of *Jagged1* and *Angiopoietin-1* [47]. In addition, Spp1 has an important role in the migration and lodgement of HSCs [48]. Double ISH analyses in this study revealed that *Spp1* co-localizes with *Tie2* and suggest that HSCs in the TB function in multiple processes, including quiescence, migration, and lodgement. Because Spp1 can bind several integrins and CD44, Spp1 may function as a stem cell adhesion molecule in hematopoietic niche cells to maintain stemness. Further analyses are required to confirm the role of Spp1 in the HSC niche.

Ctla2α is a cysteine proteinase inhibitor that was first identified by differential screening from activated T lymphocytes and mast cells [49]. The Ctla2 protein sequence is highly homologous to the pro-region of cysteine-proteases and cathepsin L. Although Ctla-4 [50] is well characterized, the function of other Ctla family members remains unclear. Ianova et al. report that both *Ctla2α* and *Ctla2α* were among 2,728 genes enriched in HSCs [12]. The expression pattern of *Ctla2α* in the bone marrow and testis suggest that it may function as a stemness regulator.

Serpina3g is a member of the serpin superfamily of protease inhibitors that regulates various physiological processes. Serpin3 was first characterized as an acute-phase plasma protease inhibitor that is widely distributed in tissues [51]. In hematopoiesis, the Serpin family plays a central role in the inhibition of HSC mobilization [52]. These data suggest that Serpina3g may have a function in HSC mobilization in the niche.

In conclusion, we have described various genes that are highly expressed in GSCs and HSCs and have confirmed their expression in each stem cell niche area (Fig. 6). These data should contribute to our understanding of stemness and provide new insight into the functions of GSCs and HSCs.

ACKNOWLEDGMENTS

The authors would like to thank Dr. Toshio Suda, Keio University, for critical reading of this manuscript. This work was supported by a grant-in-aid for Scientific Research of Japanese Society for the Promotion of Science (No.18790669).

REFERENCES

1. Weissman IL. (2000). Translating stem and progenitor cell biology to the clinic: barriers and opportunities. Science 287:1442–1446.

2. Wilson A and A Trumpp. (2006) Bone-marrow haematopoietic-stem-cell niches. Nature Rev Immunol 6:93–06.
3. Schofield R. (1978). The relationship between the spleen colony forming cell and the haematopoietic stem cell. Blood Cells 4:7–25.
4. Kiel MJ, OH Yilmaz, T Iwashita, OH Yilmaz, C Terhorst and SJ Morrison. (2005). SLAM family receptors distinguish hematopoietic stem and progenitor cells and reveal endothelial niches for stem cells. Cell 121:1109–1121.
5. Zhang J, C Niu, L Ye, H Huang, X He, WG Tong, J Ross, J Haug, T Johnson, FQ Feng, S Harris, LM Wiedemann, Y Mishina and L Li. (2003). Identification of the haematopoietic stem cell niche and control of the niche size. Nature 425:836–841.
6. Duncan AW, FM Rattis, LN DiMascio, KL Congdon, G Pazianos, C Zhao, K Yoon, JM Cook, K Willert, N Gaiano and T Reya.(2005). Integration of Notch and Wnt signaling in hematopoietic stem cell maintenance. Nature Immunol 6:314–322.
7. Willert K, JD Brown, E Danenberg, AW Duncan, IL Weissman, T Reya, JR Yates 3rd and R Nusse. (2003). Wnt proteins are lipid-modified and can act as stem cell growth factors. Nature 423:448-–452.
8. Arai F, A Hirao, M Ohmura, H Sato, S Matsuoka, K Takubo, K Ito, GY Koh and T Suda. (2004). Tie2/angiopoietin-1 signaling regulates hematopoietic stem cell quiescence in the bone marrow niche. Cell 118:149–161.
9. Antonchuk J, G Sauvageau and RK Humphries . (2002). HOXB4 induced expansion of adult hematopoietic stem cells ex vivo. Cell 109:39–45.
10. Iwama A, H Oguro, M Negishi, Y Kato, Y Morita, H Tsukui, H Ema, T Kamijo, Y Katoh-Fukui, H Koseki, M van Lohuizen and H Nakauchi. (2004). Enhanced self-renewal of hematopoietic stem cells mediated by the polycomb gene product Bmi-1. Immunity 21:843–851.
11. Ramalho-Santos M, S Yoon, Y Matsuzaki, RC Mulligan and DA Melton. (2002). "Stemness": transcriptional profiling of embryonic and adult stem cells. Science 298:597–600.
12. Ivanova NB, JT Dimos, C Schaniel, JA Hackney, KA Moore and IR Lemischka. (2002). A stem cell molecular signature. Science 298:601–604.
13. Phillips RL, RE Ernst, B Brunk, N Ivanova, MA Mahan, JK Deanehan, KA Moore, GC Overton and IR Lemischka. (2000). The genetic program of hematopoietic stem cells. Science 288:1635–1640.
14. Sharpe R. (1994). Regulation of spermatogenesis. In: *The Physiology of Reproduction*. Knobil E, JD Neill et al., eds. Raven Press, New York, pp 1363–1434.
15. Oakberg EF. (1971). Spermatogonial stem-cell renewal in the mouse. Anat.Rec 169:515–531.
16. Shinohara T, MR Avarbock and RL Brinster . (1999). b1- and a6-integrin are surface markers on mouse spermatogonial.stem cells. Proc Natl Acad Sci USA 96:5504–5509.
17. Kanatsu-Shinohara M, S Toyokuni and T Shinohara. (2004). CD9 is a surface marker on mouse and rat male germline stem cells. Biol Reprod 70:70–75.
18. Ryu BY, KE Orwig, H Kubota, MR Avarbock and RL Brinster. (2004). Phenotypic and functional characteristics of spermatogonial stem cells in rats. Dev Biol 274: 158–170.
19. Kubota H, MR Avarbock and RL Brinster. (2003). Spermatogonial stem cells share some, but not all, phenotypic and functional characteristics with other stem cells. Proc Natl Acad Sci USA 100:6487–6492.
20. Meng X, M Lindahl, ME Hyvonen, M Parvinen, DG de Rooij, MW Hess, A Raatikainen-Ahokas, K Sainio, H Rauvala, M Lakso, JG Pichel, H Westphal, M Saarma and H Sariola. (2000). Regulation of cell fate decision of undifferentiated spermatogonia by GDNF. Science 287: 1489–1493.
21. Tegelenbosch RA and DG de Rooij. (1993). A quantitative study of spermatogonial multiplication and stem cell renewal in the C3H/101 F1 hybrid mouse. Mutat Res 290:193–200.
22. Kanatsu-Shinohara M, N Ogonuki, K Inoue, H Miki, A Ogura, S Toyokuni and T Shinohara. (2003). Long-term proliferation in culture and germline transmission of mouse male germline stem cells. Biol Reprod 69:612–616.
23. Kanatsu-Shinohara M, N Ogonuki, T Iwano, J Lee, Y Kazuki, K Inoue, H Miki, M Takehashi, S Toyokuni, Y Shinkai, M Oshimura, F Ishino, A Ogura and T Shinohara. (2005). Genetic and epigenetic properties of mouse male germline stem cells during long-term culture. Development 132:4155–4163.
24. Evans MJ and MH Kaufman. (1981). Establishment in culture of pluripotential cells from mouse embryos. Nature 292:154–156.
25. Resnick JL, LS Bixler, L Cheng L and PJ Donovan. (1992). Long-term proliferation of mouse primordial germ cells in culture. Nature 359:550–551.
26. Brinster RL and MR Avarbock. (1994). Germline transmission of donor haplotype following spermatogonial transplantation. Proc Natl Acad Sci USA 91:11303–11307.
27. Fried W, W Chamberlin, WH Knospe, S Husseini and FE Trobaugh Jr. (1973). Studies on the defective haematopoietic microenvironment of Sl/Sl d mice. Br J Haematol 24:643– 650.
28. Yoshinaga K, S Nishikawa, M Ogawa, S Hayashi, T Kunisada, T Fujimoto and S Nishikawa. (1991). Role of c-kit in mouse spermatogenesis: identification of spermatogonia as a specific site of c-kit expression and function. Development 113:689– 699.
29. Fruttiger M, L Karlsson, AC Hall, A Abramsson, AR Calver, H Bostrom, K Willetts, CH Bertold, JK Heath, C Betsholtz and WD Richardson. (1999). Defective oligodendrocyte development and severe hypomyelination in PDGF-A knockout mice. Development 126:457–467.
30. Toyooka Y, N Tsunekawa, Y Takahashi, Y Matsui, M Satoh and T Noce. (2000). Expression and intracellular localization of mouse Vasa-homologue protein during germ cell development. Mech Dev 93:139–149.
31. Ogawa T, M Ohmura, Y Tamura, K Kita, K Ohbo, T Suda and Y Kubota. (2004). Derivation and morphological characterization of mouse spermatogonial stem cell lines. Arch Histol Cytol 67:297–306.
32. Kuehn MR, A Bradley, EJ Robertson and MJ Evans. (1987). A potential animal model for Lesch-Nyhan syn-

drome through introduction of HPRT mutations into mice. Nature 326:295–298.
33. Menke DB and DC Page. (2002). Sexually dimorphic gene expression in the developing mouse gonad. Gene Expr Patterns 2:359–367.
34. McLean DJ, PJ Friel, DS Johnston and MD Griswold. (2003). Characterization of spermatogonial stem cell maturation and differentiation in neonatal mice. Biol Reprod 69:2085–2091.
35. Shivdasani RA, EL Mayer and SH Orkin. (1995). Absence of blood formation in mice lacking the T-cell leukaemia oncoprotein tal-1/SCL. Nature 373:432–434.
36. Mark MP, CW Prince, T Oosawa, S Gay, AL Bronckers and WT Butler. (1987). Immunohistochemical demonstration of a 44-KD phosphoprotein in developing rat bones. J Histochem Cytochem 35:707–715.
37. Ohlstein B, T Kai, E Decotto and A Spradling. (2004). The stem cell niche: theme and variations. Curr Opin Cell Biol 16:693–699.
38. Wistow GJ and J Piatigorsky. (1988). Lens crystallins: the evolution and expression of proteins for a highly specialized tissue. Annu Rev Biochem 57:479–504.
39. Bhat SP and CN Nagineni. (1989). alpha B subunit of lens-specific protein alpha-crystallin is present in other ocular and non-ocular tissues. Biochem Biophys Res Commun 158:319–325.
40. Morrison LE, HE Hoover, DJ Thuerauf and CC Glembotski. (2003). Mimicking phosphorylation of alphaB-crystallin on serine-59 is necessary and sufficient to provide maximal protection of cardiac myocytes from apoptosis. Circ Res 92:203–211.
41. de Rooij DG, M Okabe and Y Nishimune. (1999). Arrest of spermatogonial differentiation in jsd/jsd, Sl17H/Sl17H, and cryptorchid mice. Biol Reprod 61:842–847.
42. Haylock DN and SK Nilsson. (2006). Osteopontin: a bridge between bone and blood. Br J Haematol 134:467–474.
43. de Rooij DG and JA Grootegoed. (1998). Spermatogonial stem cells. Curr Opin Cell Biol 10:694–701.
44. McLaren A. (2003). Primordial germ cells in the mouse. Dev Biol 262:1–15.
45. Fujino RS, Y Ishikawa, K Tanaka, M Kanatsu-Shinohara, K Tamura, H Kogo, T Shinohara and T Hara. (2006). Capillary morphogenesis gene (CMG)-1 is among the genes differentially expressed in mouse male germ line stem cells and embryonic stem cells. Mol Reprod Dev 73:955–966.
46. Kurosaki H, Y Kazuki, M Hiratsuka, T Inoue, Y Matsui, CC Wang, M Kanatsu-Shinohara, T Toda and M Oshimura. (2007). A comparison study in the proteomic signatures of multipotent germline stem cells, embryonic stem cells, and germline stem cells. Biochem Biophys Res Commun 353:259–267.
47. Stier S, Y Ko, R Forkert, C Lutz, T Neuhaus, E Grunewald, T Cheng, D Dombkowski, LM Calvi, Sr Rittling and DT Scadden. (2005). Osteopontin is a hematopoietic stem cell niche component that negatively regulates stem cell pool size. J Exp Med 201:1781–1791.
48. Nilsson SK, HM Johnston, GA Whitty, B Williams, RJ Webb, DT Denhardt, I Bertoncello, LJ Bendall, PJ Simmons and DN Haylock. (2005). Osteopontin, a key component of the hematopoietic stem cell niche and regulator of primitive hematopoietic progenitor cells. Blood 106:1232–1239.
49. Denizot F, JF Brunet, P Roustan, K Harper, M Suzan, MF Luciani, MG Mattei and P Golstein. (1989). Novel structures Ctla2α and CTLA-2β expressed in mouse activated T cells and mast cells and homologous to cysteine proteinase proregions. Eur J Immunol 19:631–635.
50. Teft WA, MG Kirchhof and J Madrenas. (2006). A molecular perspective of CTLA-4 function. Annu Rev Immunol 24:65–97.
51. Dickson I and CA Alper. (1974). Changes in serum proteinase inhibitor levels following bone surgery. Clin Chim Acta 54:381–385.
52. Winkler IG, J Hendy, P Coughlin, A Horvath and JP Levesque. (2005). Serine protease inhibitors serpina1 and serpina3 are down-regulated in bone marrow during hematopoietic progenitor mobilization. J Exp Med 201: 1077–1088.

Address reprint requests to:
Dr. Isao Hamaguchi
Department of Safety Research on Blood and Biological Products
National Institute of Infectious Diseases
4-7-1, Gakuen, Musashimurayama
Tokyo, 208-0011, Japan

E-mail: 130hama@nih.go.jp

Received for publication May 2, 2007; accepted after revision August 2, 2007.

Available online at www.sciencedirect.com
ScienceDirect
Vaccine 25 (2007) 3355–3364
Vaccine
www.elsevier.com/locate/vaccine

Two vaccine toxicity-related genes Agp and Hpx could prove useful for pertussis vaccine safety control

Isao Hamaguchi [a,1], Jun-ichi Imai [b,1], Haruka Momose [a,1], Mika Kawamura [b,d], Takuo Mizukami [a], Hiroshi Kato [a], Seishiro Naito [a], Jun-ichi Maeyama [a], Atsuko Masumi [a], Madoka Kuramitsu [a], Kazuya Takizawa [a], Masayo Mochizuki [a], Masaki Ochiai [c], Akihiko Yamamoto [c], Yoshinobu Horiuchi [c], Nobuo Nomura [e], Shinya Watanabe [b], Kazunari Yamaguchi [a,*]

[a] *Department of Safety Research on Blood and Biological Products, National Institute of Infectious Diseases, 4-7-1 Gakuen, Musashimurayama, Tokyo 208-0011, Japan*
[b] *Department of Clinical Informatics, Tokyo Medical and Dental University, Tokyo, Japan*
[c] *Department of Bacterial Pathogenesis and Infectious Control, National Institute of Infectious Diseases, 4-7-1 Gakuen, Musashimurayama, Tokyo 208-0011, Japan*
[d] *Medicrome, Inc., Sendagaya, Shibuya-ku, Tokyo 151-0051, Japan*
[e] *Biological Information Research Center, National Institute of Advanced Industrial Science and Technology, Japan*

Received 31 July 2006; received in revised form 21 December 2006; accepted 28 December 2006
Available online 16 January 2007

Abstract

Conventional animal tests such as leukocytosis promoting tests have been used for decades to evaluate toxicity of pertussis vaccine. Here, we examined gene expression in relation to the vaccine toxicity using a DNA microarray. Comparison of conventional animal test data with the DNA microarray-based gene expression data revealed a gene expression pattern highly correlated with leukocytosis in animals. Of 10,490 rat genes analyzed, two genes, α1-acid-glycoprotein (Agp) and hemopexin (Hpx), were found up-regulated by the toxin administration in a dose-dependent manner (assayed by a quantitative PCR based on the microarray). Variation of the gene expression was very small amongst the test animals, and the results were highly reproducible. These findings suggest that gene expression analysis of vaccine-treated animals can be used as an accurate and simple method of pertussis vaccine safety assessment.

Keywords: Pertussis vaccine; Microarray; Quantitative RT-PCR; Agp; Hpx; Safety test; Pertussis toxin

1. Introduction

Although regarded as one of the great public health successes, vaccines are not absolutely safe. While most adverse events associated with vaccines are minor and self-limiting, some vaccines have been associated with rare but serious health consequences.

Pertussis, or whooping cough, is an acute infectious disease caused by the bacterium *Bordetella pertussis*, which was first isolated in 1906 [1]. Outbreaks of pertussis were first described in the 16th century [2], and in the 20th century, pertussis was one of the most common childhood diseases and a major cause of childhood mortality. Prior to the availability of whole-cell pertussis vaccine in the 1940s, annual morbidity of pertussis exceeded 200,000 cases. Pertussis vaccine has long been used in many countries as the effective protective measure against the disease, leading to a dramatically decreased incidence of the disease.

* Corresponding author. Tel.: +81 42 561 0771.
E-mail address: kyama@nih.go.jp (K. Yamaguchi).
[1] These authors contributed equally to this work.

0264-410X/$ – see front matter © 2007 Elsevier Ltd. All rights reserved.
doi:10.1016/j.vaccine.2006.12.059